SUBHARMONIC RESONANCE IN A LIMIT CYCLING VOLTAGE REGULATOR

by

Mehmet Ali Güler

United States
Naval Postgraduate School

THESIS

SUBHARMONIC RESONANCE IN A LIMIT CYCLING VOLTAGE REGULATOR

by

M. Ali Güler

December 1970

Subharmonic Resonance in a Limit Cycling Voltage Regulator

by

M. Mehmet Ali Güler
Lieutenant (junior grade), Turkish Navy
B.S., Naval Postgraduate School, 1970

Submitted in partial fulfillment of the
requirements for the degree of

MASTER OF SCIENCE IN ELECTRICAL ENGINEERING

from the

NAVAL POSTGRADUATE SCHOOL
December 1970

ABSTRACT

In practice, thyristor rectifiers are used as high current-low voltage power supplies. Under certain conditions such rectifiers introduce subharmonic resonances.

In this paper, a limit cycling voltage regulator system is simulated in the digital computer. The reference voltage and load are varied and the system gain is changed for better understanding of their effects on the subharmonics. A Fourier analysis of the output wave shape then determined the existence and amplitude of subharmonic components.

TABLE OF CONTENTS

LIST OF TABLES

Tables

LIST OF DRAWINGS

ACKNOWLEDGEMENT

The author wishes to express his appreciation to Dr. G. J. Thaler for the invaluable assistance and counsel which he has offered during the preparation of this thesis.

I. LIMIT CYCLING SYSTEMS, THEORY OF OPERATION

A. INTRODUCTION TO LIMIT CYCLING SYSTEM

In practice, it might be required to have a control system which will generate a limit cycle. In this thesis the goal is to investigate the characteristics of a limit cycling voltage regulator. This kind of voltage regulator system is potentially useful as a low cost source of well regulated direct current.

The system introduced in this paper has linear and nonlinear elements. One of the tools for linearizing nonlinear systems is the describing function method. In dealing with limit cycling systems the ordinary describing function method predicts the limit cycle, but is not adequate for a complete analysis. The Dual input describing function is a useful method for investigation of the limit cycling system when subharmonic resonances are anticipated.

B. DUAL INPUT DESCRIBING FUNCTION (DIDF)

West (4), introduced a new mathematical device which is called the "Dual input Describing function" (DIDF). It is an extension of the conventional describing function which linearizes the nonlinearity when forced by two inputs.

The Dual input Describing function is a very powerful tool for the investigation of limit cycling systems. It will be used for prediction of subharmonic resonance.

For better understanding of a limit cycling system a general block diagram is introduced in Figure 1-1a. In this limit cycling control system $N(A,\omega)$ represents the nonlinear element, $G(j\omega)$ the linear element. The DIDF is based on the error input to the nonlinear element. For a well designed system the error X(t), is equal to

$$X(t) = r(t)-C(t)$$

and would be small so that any limit cycling period To, can be modeled as shown on Figure 1-1b. In this model the sinusoid amplitude A is associated with one input and the D.C bias amplitude is associated with the second input. Then the input to the nonlinear element is

$$X(t) = B+A\sin\theta$$

Now, the calculation of the DIDF for the nonlinear element $N(a,\omega)$, is accomplished by computing the ratio of the output amplitude spectrum of the nonlinearity to its input which gives two DIDF.

$$N_o(A,B) = \frac{A'}{A} e^{-j\theta}$$

and

$$N_s(A,B) = \frac{B'}{B}$$

The first nonlinearity is considered as limit cycle DIDF and will be used to predict the system limit cycle. The second DIDF is considered as a linear gain for range B/A and leads to linear system description due to input. The

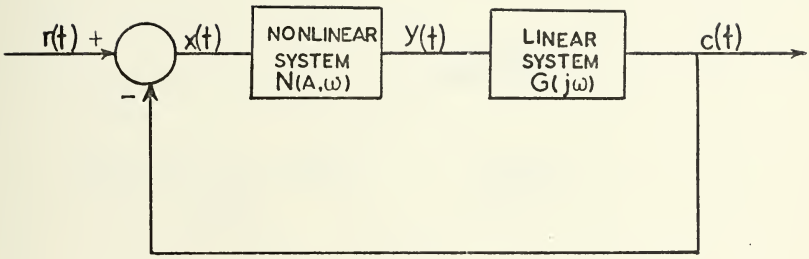

FIGURE 1.1a. Basic limit cycling system.

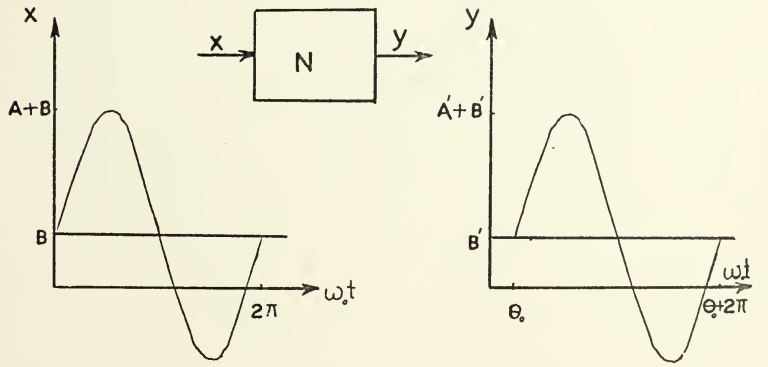

FIGURE 1.1b. Representation of input-output relation of a nonlinear element.

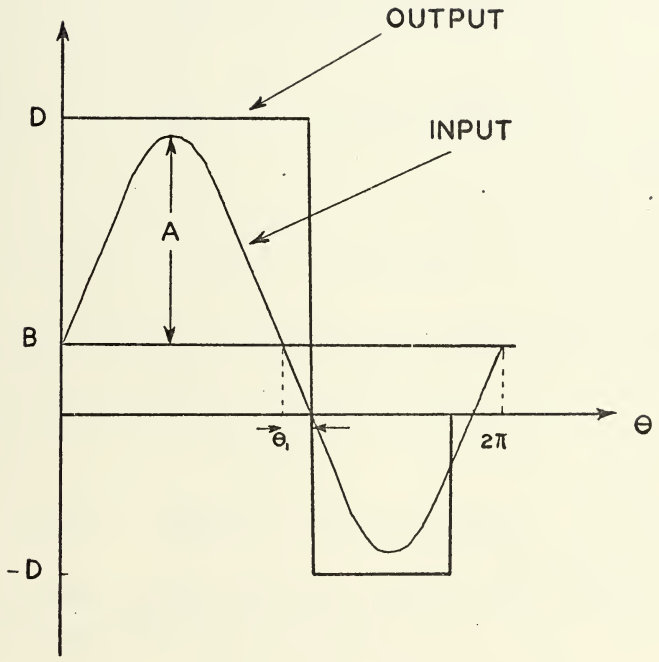

FIGURE 1.1c. Input and output wave form for an ideal relay.

mathematical definition of both DIDF's follow directly from Fourier analysis and they can be written as

$$N_o(A,B) = Re[N_o(A,B)]+\dot{J}I_m[N_o(A,B)]$$

$$= \frac{1}{\pi A}\int_0^{2\pi} y(B+A\sin\theta)\sin\theta d\theta$$

$$+ \frac{J}{\pi A}\int_0^{2\pi} y(B+A\sin\theta)\cos\theta d\theta \qquad (1\text{-}1)$$

and

$$N_s(A,B) = \frac{1}{2\pi B}\int_0^{2\pi} y(B+A\sin\theta)d\theta \qquad (1\text{-}2)$$

Equation (1-1) can be reduced since integration of the cosine term of $N_o(A,B)$ in this interval is zero. Then the simplified form of $N_o(A,B)$ can be written as

$$N_o(A,B) = \frac{1}{2\pi B}\int_0^{2\pi} y(B+A\sin\theta)\sin\theta d\theta \qquad (1\text{-}3)$$

In the limit cycling system B/A will be small and an incremental DIDF can be derived as $B\to o$

$$DIDF \triangleq \lim_{B\to o}[N_s(A,B)]$$

and

$$DIDF = \frac{1}{2\pi}\lim_{B\to o}\left[\frac{1}{B}\int_0^{2\pi} y(B+A\sin\theta)d\theta\right] \qquad (1\text{-}4)$$

C. DIDF FOR IDEAL RELAY

Let us consider an ideal relay with drive levels ±D, Figure 1.1c. There the input to the nonlinearity is

$$X = B+A\sin\omega_0 t$$

$$= B+A\sin\theta$$

The ideal relay has a single valued nonlinearity, therefore, computation of the limit cycle DIDF is done by using the result obtained in equation (1-3) and applying it to Figure 1.1c. Then the DIDF can be written

$$N_o(A,B) = \frac{1}{\pi A}\int_0^{2\pi} y(B+A\sin\theta)\sin\theta d\theta$$

$$= \frac{1}{\pi A}\left[\int_0^{\pi+\theta_1} D\sin\theta d\theta + \int_{\pi+\theta_1}^{2\pi-\theta_1} (-D)\sin\theta d\theta + \int_{2\pi-\theta_1}^{2\pi} D\sin\theta d\theta\right]$$

$$= \frac{4D}{\pi A}\cos\theta_1$$

and

$$\theta_1 = \sin^{-1}(B/A)$$

$$N_o(A,B) = \frac{4D}{\pi A}\sqrt{1-(B/A)^2} \qquad (1\text{-}5)$$

The DIDF, associated with the signal is

$$N_s(A,B) = \frac{1}{2\pi B}\left[\int_{o}^{\pi+\theta_1} D\,d\theta \int_{\pi+\theta_1}^{2\pi-\theta_1} (-D)\,d + \int_{2\pi-\theta_1}^{2\pi} D\,d\theta\right]$$

$$= \frac{2D}{\pi B}\,\theta_1$$

$$= \frac{2D}{B}\,\sin^{-1}(B/A) \qquad (1\text{-}6)$$

If $B \to o$, forumla (1-6) can be written

$$N_s(A,B) = \lim_{B\to o}[N_s(A,B)]$$

$$N_s(A,B) = \frac{2D}{\pi A} \qquad (1\text{-}7)$$

And the DIDF for two sinusoids input is found as:

$$X = A\sin(\omega_o t+\theta)+B\sin\omega_s t$$

in which ω_o is the limit cycle frequency and ω_s is the signal frequency. Then the DIDF will be

$$N_o(A,B) = \frac{4D}{\pi A}\left[1-\frac{1}{4}\left(\frac{B}{A}\right)^2 - \frac{3}{64}\left(\frac{B}{A}\right)^4\cdots\right] \qquad (1\text{-}8)$$

$$N_s(A,B) = \frac{2D}{\pi}\left[1+\frac{1}{8}\left(\frac{B}{A}\right)^2 + \frac{3}{64}\left(\frac{B}{A}\right)^4+\cdots\right] \qquad (1\text{-}9)$$

If this result is compared with the approximate DIDF, it can be said that the approximate DIDF which is derived as equation (1-5), (1-6) are valid for 5 percent accuracy but if the following conditions are satisfied:

$$\frac{B}{A} < \frac{1}{3}$$

$$\frac{\omega_s}{\omega_o} < \frac{1}{3} \qquad (1\text{-}10)$$

Then it is possible to have 2.5 percent accuracy with respect to the exact DIDF.

Therefore, for the ideal relay case the limit cycle DIDF are always valid to better than 5 percent accuracy referred to the exact DIDF, under the restriction of (1-10).

D. LIMIT CYCLING SYSTEM CHARACTERIZATION

The system here considered is a kind of system which always has a limit cycle. Most limit cycling systems include a pre-filter like that shown in Figure 1.2. The fundamental purpose of this filter is to reshape the command signal amplitude to the input such that at the input of the nonlinearity inequalities (1-10) are satisfied. This brings a design problem of the pre-filter which will not be considered in this thesis.

1. Frequency Domain Description

To investigate sinusoidal frequency analysis of limit cycling systems, the system model is illustrated in Figure 1.2. r(t) is a sinusoid and the input to the nonlinearity N is

$$X = A\sin(\omega_o t+\theta)+B\sin\omega_s t$$

The goal here is to investigate the interaction between two sinusoids, through the nonlinearity and differents inputs

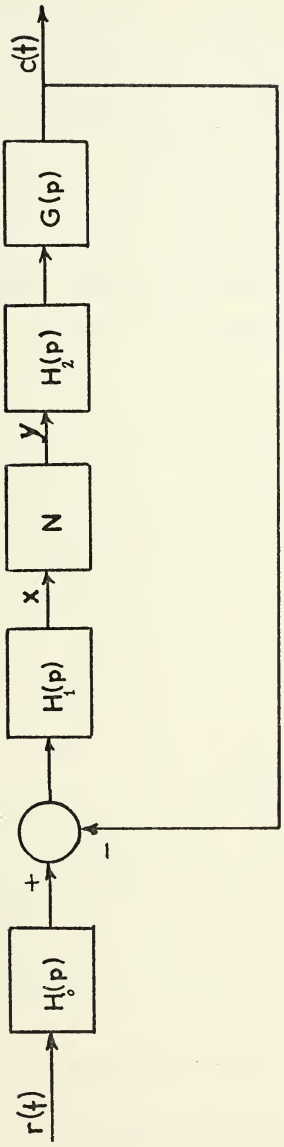

FIGURE 1.2. Basic limit cycling system structure.

are considered in this analysis. Figure 1.3 shows the range of possibilities of the signal and limit cycle. For Figure 1.3a the output through the nonlinearity is nearly sinusoidal at the limit cycle frequency but is phase shifted with respect to the limit cycle. It can be said that signal through relay is zero which means $N_s=0$. Also it may be said that for signal frequency greater than the limit cycle frequency but satisfying the amplitude ratio condition also gives $N_s=0$.

In Figure 1.3b the amplitude ratio is satisfied but the frequency ratio is 0.5. In this case the signal through the nonlinearity would not lose identity and the amplitude ratio only will depend on the phase shift of the input component to the nonlinearity. Then for the case shown in Figure 1.3b, it can be concluded that $N_s=N_s(\theta)$. For a frequency ratio equal to 0.33, N_s affects the input signal amplitude by factor of 16 percent and a phase of 4 degrees. For a frequency ratio greater than 0.33, (but amplitude ratio satisfied) N_s can be considered independent of relative time position since the change in amplitude and phase ratio are never greater than 1 percent. Therefore as a result of these conclusions the open loop transfer function can be written as

$$G_{eq}(j\omega)=N_s.H_{eq}.G(j\omega) \quad \text{for } |\omega|<\frac{\omega_o}{3}$$

$$G_{eq}(j\omega)=\gamma.N_s.H_{eq}.G(j\omega) \quad \text{for } \frac{\omega_o}{3}\leq|\omega|<\omega_o$$

$$G_{eq}(j\omega)=0 \quad \text{for } \omega_o<|\omega| \qquad (1\text{-}11)$$

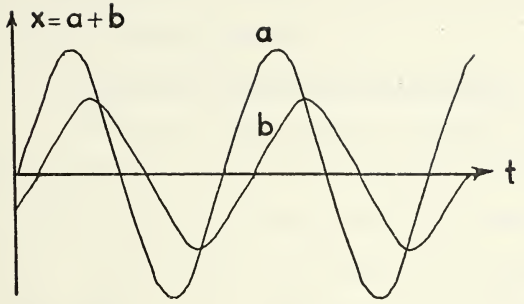

FIGURE 1.3a. AR = 0.33, FR = 1.00

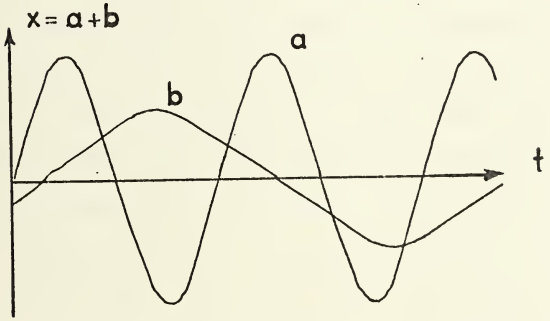

FIGURE 1.3b. AR = 0.33, FR = 0.5

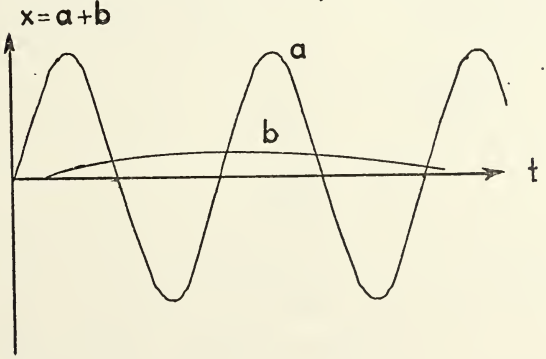

FIGURE 1.3c. AR = 0.33, FR = 0.16

FIGURE 1.3. Range of possibilities of input.

where γ represents a complex number depending on the relative phase of these signals.

2. Pole-Zero System Characterization

Frequency domain analysis shows that in the range between $-\omega_o/3<\omega_s<\omega_o/3$ rad/sec along the imaginary axis, if the amplitude ratios are also satisfied the system behaves linearly. In the ranges $\omega_o/3\leq\omega_s\leq\omega_o$ and $-\omega_o\leq\omega_s\leq\omega_o/3$ rad/sec the signal gain of the nonlinearity is a function of time, and for the remaining portion of the $j\omega$ axis, the signal gain is always zero. Now, consider exponentials for which the amplitude ratio is satisfied, (amplitude ratio refers to ratio of peak exponential to peak limit cycle amplitude) it may be noted that the exponential excited output of a relay is relatively independent of the time origin of the input exponential signal in the existence of the limit cycle, if the signal lasts for two or more limit cycle periods Figure 1.4 shows this situation. Then, the minimum value of the input time constant is,

$$4\tau_{min} \simeq 2 \left(\frac{2\pi}{\omega_o}\right)$$

$$\frac{1}{\tau_{min}} \simeq \frac{\omega_o}{3}$$

Then, the pole-zero configuration of the system may be described. Consider the complex plane "p" to be divided into three regions, shown in Figure 1.5.

The nonlinear element N of the system will be considered as a gain element and N is derived for the relay,

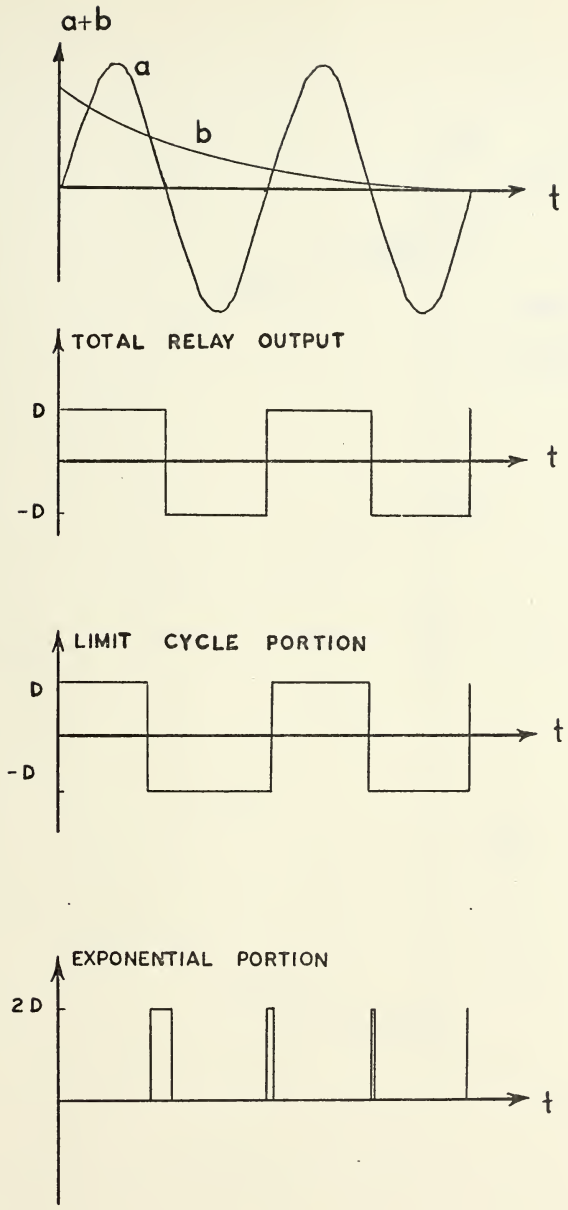

FIGURE 1.4. Response of ideal relay in the presence of limit cycle.

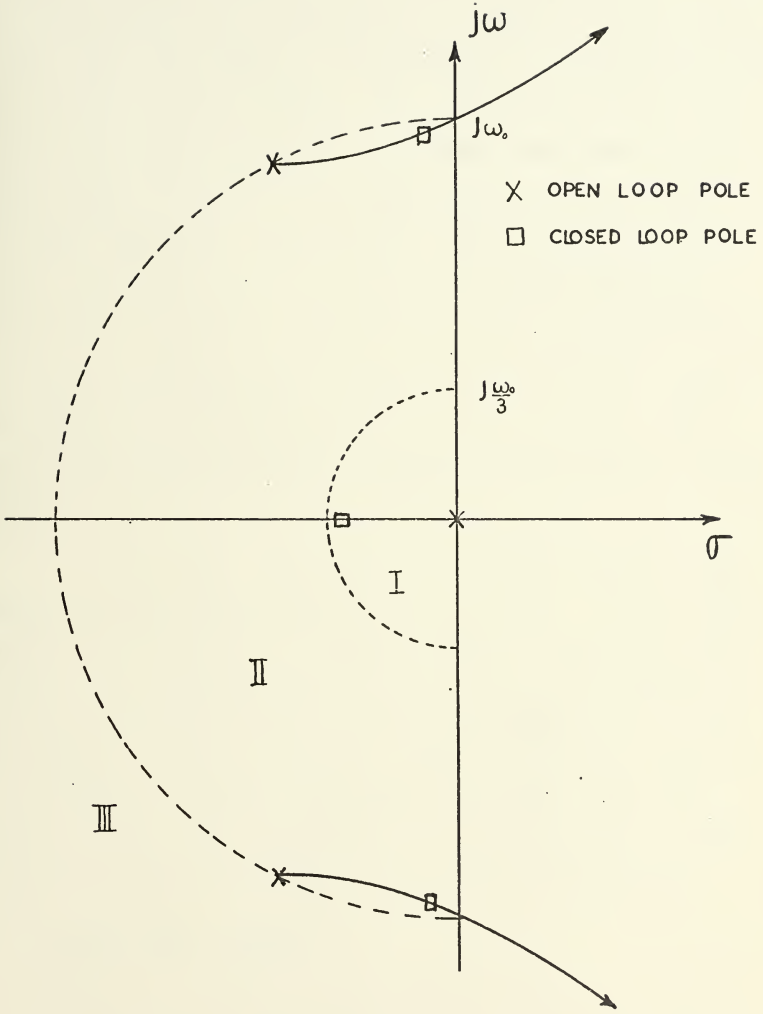

FIGURE 1.5. Root locus plot for G(p).

therefore, it will not contain any phase shifting. If the open loop system gain is adjusted to one-half of the value of the limit cycle gain, it is possible to automatically obtain a limit cycling system. The closed loop roots of the system can be approximately determined, such that, if the gain at the crossover of the imaginary axis $N=N_o$ which is the limit cycle gain, and at gain value of $N=N_o/2=N_s$ one of the closed loop roots will be close to the intercept point of the $\omega_o/3$ circle on the real axis which is shown as P_a. $P_a \simeq \omega_o/3$ and the other complex pair of roots would be very close to the circumference of the ω_o circle. This result determines the dynamic response of the limit cycling system.

One of the important points about limit cycling systems is from the stability point of view: if the sensitivity of the system is increased then the limit cycle amplitude increases but the gain N_s decreases and always the $S.N_s$ product remains constant. Closed loop root locations do not change, only the limit cycle amplitude will be changed. Also, it is possible to have instability in the system but may be the system response does not change.

E. CLOSED LOOP PROPERTY

Consider a limit cycling system as shown in Figure 1.2. Then the open loop transfer function of the system is

$$G_{eq}(p) = N_s.H_1(p).H_2(p).G(p)$$
$$= N_s.H_{eq}.G(p) \qquad (1\text{-}12)$$

The DIDF for the ideal relay were found in equations (1-5) and (1-6) and they may be approximated as,

$$N_o \simeq \frac{4D}{\pi A}$$

$$N_s \simeq \frac{2D}{\pi A}$$

and the ratio of these two,

$$\frac{N_s}{N_o} \simeq \frac{1}{2}$$

then N_s may be written in equation (1-12)

$$G_{eq}(j\omega) = N_s . H_{eq} . G(j\omega)$$

$$= \frac{1}{2} N_o . H_{eq} . G(j\omega)$$

in order to sustain the limit cycle

$$N_o . H_{eq} . G(j\omega) = -1 \qquad (1\text{-}13)$$

must be satisfied. Then,

$$G_{eq}(j\omega) = -\frac{1}{2} \qquad (1\text{-}14)$$

This is a kind of proof of the explanation given earlier for open loop gain of limit cycling systems.

II. PERFORMANCE CHARACTERISTICS OF THE LIMIT CYCLING VOLTAGE REGULATOR

A. SYSTEM DESCRIPTION

The block diagram of the voltage regulator system used in this thesis is shown in Figure 2.1. The complete circuit diagram is shown in Appendix A.

The firing circuit, instead of using a separate circuit for each thyristor uses a relay to turn all thyristors on or off. If the relay is on a positive voltage is applied to all thyristor gates and this causes conduction in the rectifier. If the relay is off then the rectifiers will not conduct.

The rectifier unit is a three phase full-wave rectifier made of a combination of six thyristors. The thyristor is a solid state device which is equivalent to a thyratron. One thyristor device is a silicon controlled rectifier. It is a four layer device and may be likened to a PNP transistor joined to an NPN transistor and sharing a common collector-base junction. The thyristor and the characteristic curve of the thyristor are shown in Figure 2.2.

As a load unit, a second order filter with very low damping factor is used. It is an LCR filter. The values of L,C are constant and variation of the damping ratio is obtained by varying the load resistance.

The system has a nonlinearity due to the relay and the thyristor characteristics provide a second nonlinearity.

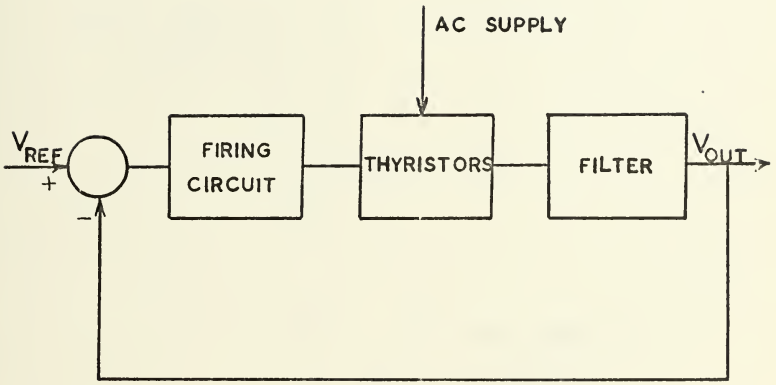

FIGURE 2.1. Basic block diagram of the limit cycling voltage regulator.

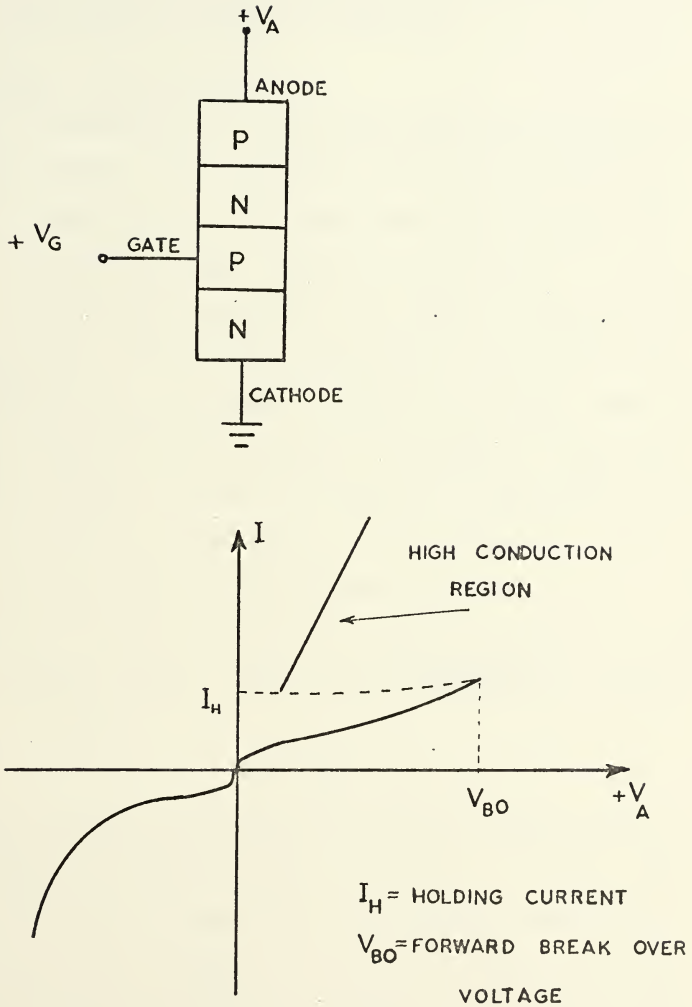

FIGURE 2.2. Thyristor characteristic.

These two nonlinearities are treated as one nonlinearity in analysis of the system, providing the simplified block diagram of the system as shown in Figure 2.3.

B. STEADY STATE ACCURACY

It is important to investigate the system response to different inputs. For this purpose the voltage regulator system is analyzed for a load resistance R=0.8Ω, and different reference voltages applied to the system. The important feature to be studied is the output characteristic of the system. For different reference voltages the outputs obtained were subjected to Fourier analysis. Table 2-1 shows the result of this analysis. In Table 2-1 results taken from digital computer calculation of the Fourier series and subroutine FORIT used for this analysis. In the Table 2-1 A_o is the DC value of the output.

These results show that the system output is not equal to the required value. Then the difference may be defined as α,

$$\alpha = V_{ref} - A_o$$

For high reference voltages the system has large α and if V_{ref} gradually decreases, α also decreases. At V_{ref} = 52 volt α changes it's sign, that is, for low voltage cases the system output voltage is a little bit higher than V_{ref}. This may be good but when V_{ref} decreases the system ripple instability increases which is not desired for the system. The numerical results show that if V_{ref} is decreased gradually,

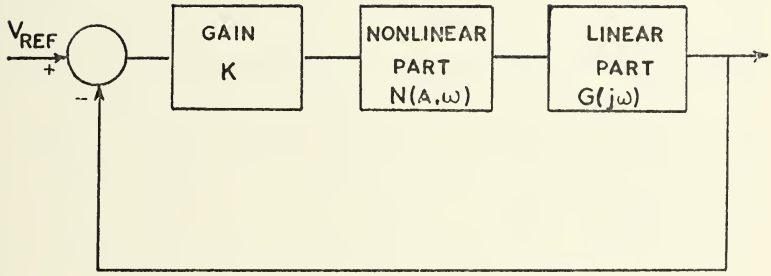

FIGURE 2.3. Simplified block diagram of the limit cycling voltage regulator.

FOURIER ANALYSIS FOR R=0.8Ω

REFERENCE VOLTAGE V_{REF} (VOLT)	A_o (VOLT)	LIMIT CYCLE AMPLITUDE (VOLT)	SUBHARMONIC AMPLITUDE (VOLT)	LIMIT CYCLE FREQUENCY (Hz)	SUBHARMONIC FREQUENCY (Hz)	ORDER OF SUBHARMONIC
64	60.589	3.34	---	36.4	---	1/2
62	59.685	2.82	0.373	36.4	18.2	1/2
60	59.111	2.36	---	40.0	---	1/2
58	57.24	2.07	0.146	51.6	25.8	1/2
56	56.277	2.4	0.121	51.2	25.6	1/2
54	53.961	1.53	0.134	72.4	36.2	1/2
52	52.966	2.21	0.133	60.4	30.2	1/2
50	50.272	1.24	0.143	90.0	45.0	1/2
48	49.181	1.505	0.475	56.2	28.1	1/2
46	47.497	1.41	0.635	68.4	17.1	1/4

TABLE 2-1

subharmonics become more effective and this may make the system unstable. For V_{ref} = 58 volt, the amplitude of the subharmonic is quite small (about 0.146 volt) but for V_{ref} = 46 volt, the subharmonic amplitude becomes 0.635 volt which is quite large compared with 0.146 volt. Also the results show that the limit cycle amplitude shows an opposite reaction. Increase in the subharmonics amplitudes caused a decrease in limit cycle amplitude. Figure 2.4 shows the output of the voltage regulator at V_{ref} = 60 volt and V_{ref} = 58 volt.

C. TRANSIENT RESPONSE OF THE SYSTEM

For investigation of the transient response of the system only the linear parts are taken into account. The behavior of the nonlinear part is not considered. The linear filter of the system is assumed to be as shown in Figure 2.5. And the transfer function of the system is

$$G(S) = \frac{Vout}{Vin} = \frac{1/LC}{S^2+(1/RC)S+(1/LC)} \qquad (2\text{-}1)$$

In general second order system characteristic equations can be written in the form

$$S^2+2\xi\omega_n S+\omega_n{}^2 = 0$$

then for the filter,

$$\omega_n = \frac{1}{\sqrt{LC}} \qquad \text{and} \qquad \xi = \frac{1}{2R}\sqrt{\frac{L}{C}}$$

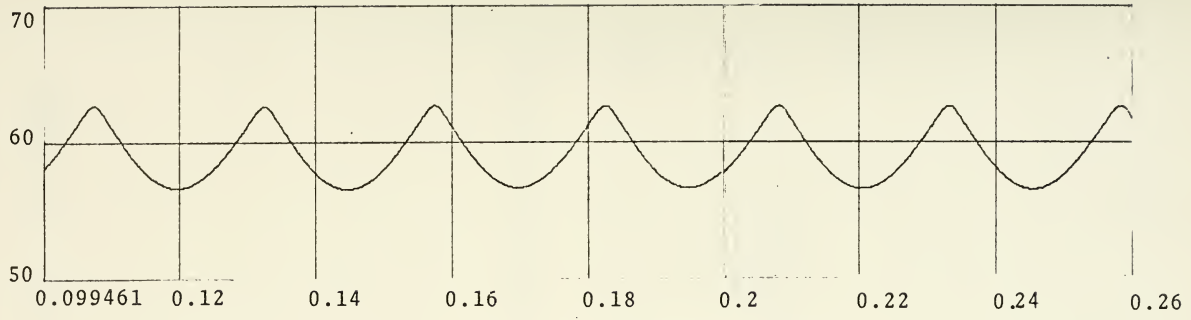

FIGURE 2.4a. Output waveform: V_{ref} = 60V., R = 0.8Ω

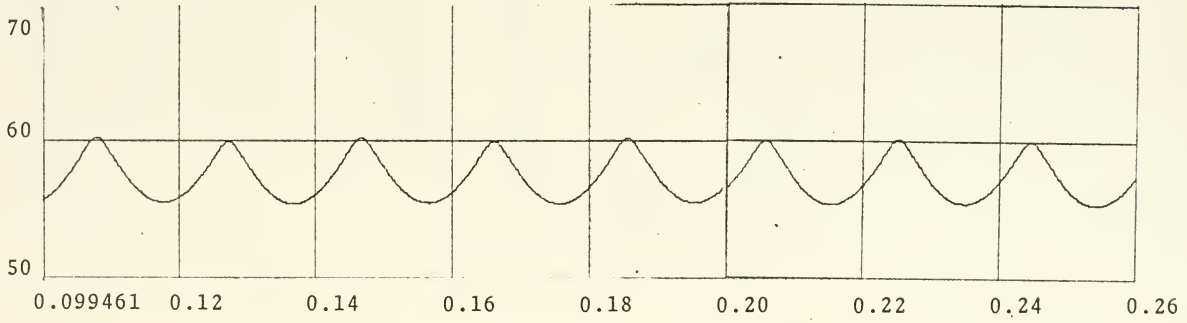

FIGURE 2.4b. Output waveform: V_{ref} = 58V., R = 0.8Ω

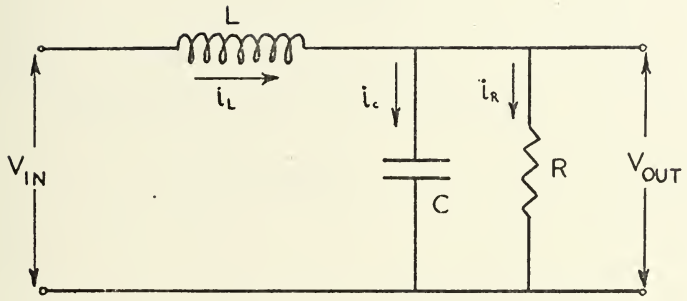

FIGURE 2.5. Filter and load of the system.

During analysis of the system L and C are held constant and only the value of R is changed

$$C = 0.1f.$$

$$L = 0.0005h.$$

therefore,

$$\omega_n = 141 \text{ rad/sec}$$

and for $R = 0.8\Omega$

$$\xi = 0.044194$$

which is a very low damping factor.

The settling time of the filter is

$$t_s = \frac{4}{\xi\omega_n}$$

Then,

$$t_s = 2.5 \quad \text{sec for } R = 3.2\Omega$$

$$t_s = 1.23 \quad \text{sec for } R = 1.6\Omega$$

$$t_s = 0.645 \text{ sec for } R = 0.8\Omega$$

The filter transfer function can be written in Bode form,

$$G(j\omega) = \frac{1}{LC(j\omega)^2+L/R(j\omega)+1}$$

And for $R = 0.8\Omega$

$$G(j\omega) = \frac{1}{(1/2\ 10^4)(j\omega)^2+(12.3/2\ 10^4(j\omega)+1} \qquad (2\text{-}2)$$

The phase and amplitude curves of the Bode diagram are drawn with the IBM-360 digital computer and the curves are

illustrated in Figure 2.6. The analysis of the closed loop characteristic of the filter is shown on the Nichols plot in Figure 2.7.

D. PREDICTION OF LIMIT CYCLES

For prediction of the limit cycle frequency, the basic describing function method is used. The describing function for the nonlinearity of the system which includes relay and rectifier is derived by Leszcynski (Ref. 15). And for the linear part of the system for this prediction equation (2-2) is used. Figure 2.8 and Figure 2.9 shows the Nichols plot of the limit cycling voltage regulator for V_{ref} = 64 volt and V_{ref} = 62 volt both at R = 0.8Ω. Figure 2.8 gives the limit cycle frequency f_{lc} = 35HZ and limit cycle amplitude B = 3.6544 volt. This agrees with the experimental result shown in Table 2-1. Also for V_{ref} = 62 volt the Nichols chart of Figure 2.9 gave the limit cycle frequency f_{lc}=37HZ and limit cycle amplitude about B = 2.4632 volt. Experimental results in Table 2-1 gives f_{lc} = 36.4HZ and limit cycle amplitude about B = 2.82 volt which agree fairly well with the result obtained by Nichols plot.

E. SUBHARMONICS

One of the purposes of this paper is also to investigate subharmonic resonances in the system. Table 2-1 for Fourier analysis shows relationships between V_{ref} and the subharmonic amplitude and frequency. Results show that changes in V_{ref} affect subharmonic amplitudes. If V_{ref} is increased the subharmonic amplitudes also increase and for

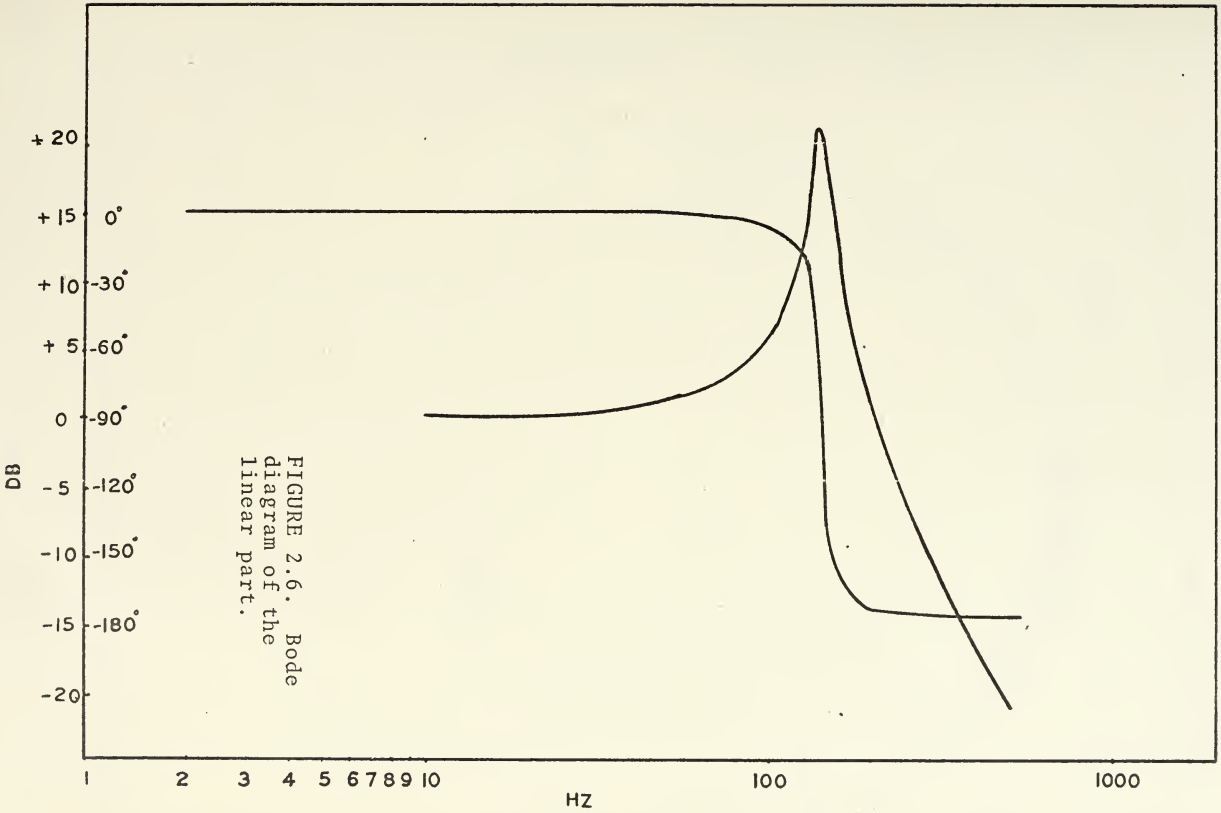

FIGURE 2.6. Bode diagram of the linear part.

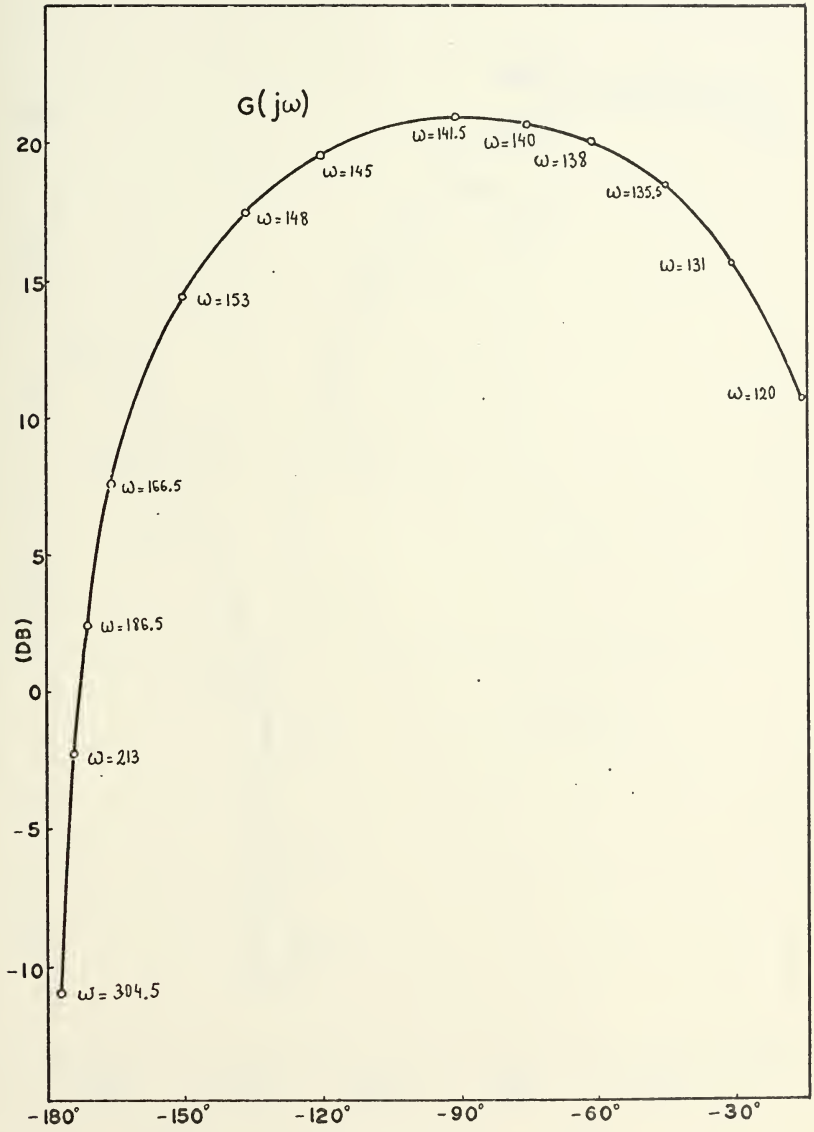

FIGURE 2.7. Nichols plot of the filter for R = 0.8Ω.

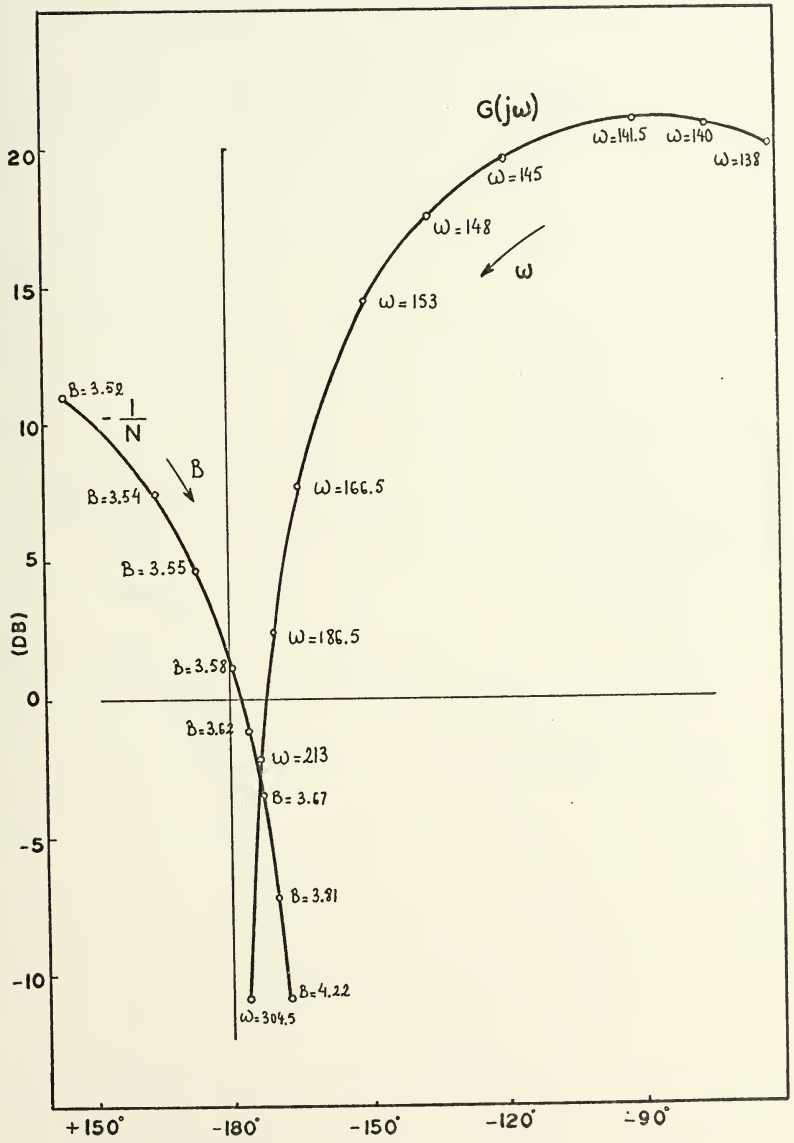

FIGURE 2.8. Nichols plot of system for V_{ref}= 64V., R=0.8Ω, f_{lc}=35.

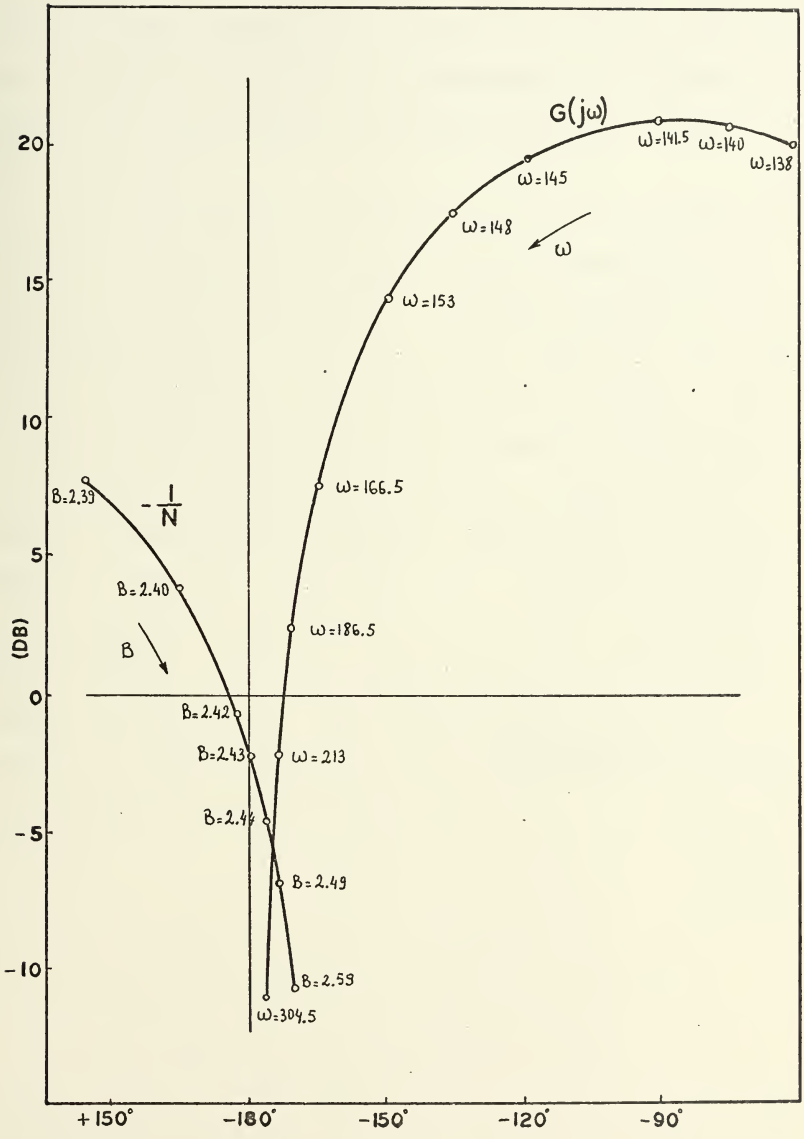

FIGURE 2.9. Nichols plot of the system for V_{ref}=62V., R=0.8Ω, f_{1c} = 37 HZ.

$V_{ref} \leq 50$ volt subharmonics become very important. System behavior gives a ripple instability at the output. This instability may be caused by the high amplitude subharmonics. Figure 2.10 shows this kind of output for $V_{ref} = 48$ and $V_{ref} = 46$ volt.

From the frequency response point of view, it may be concluded that changes in V_{ref} do affect appreciably the frequency of the subharmonics. The basic frequency of the subharmonic tends to remain at 25 cps. Table 2-1 shows that changes in the system load resistance; R = 0.8Ω, R = 1.6Ω, R = 3.2Ω caused no change in the subharmonic frequency and in like manner changes in the reference voltage did not change the subharmonic frequency. These results shown in Table 5-1, Table 5-2, and Table 5-3. It may be concluded that any change in the system will not effect the subharmonic frequency since the system forced the subharmonics toward the 25 HZ value. But the amplitude of the subharmonic is quite sensitive to any change in the system or any disturbance to the system.

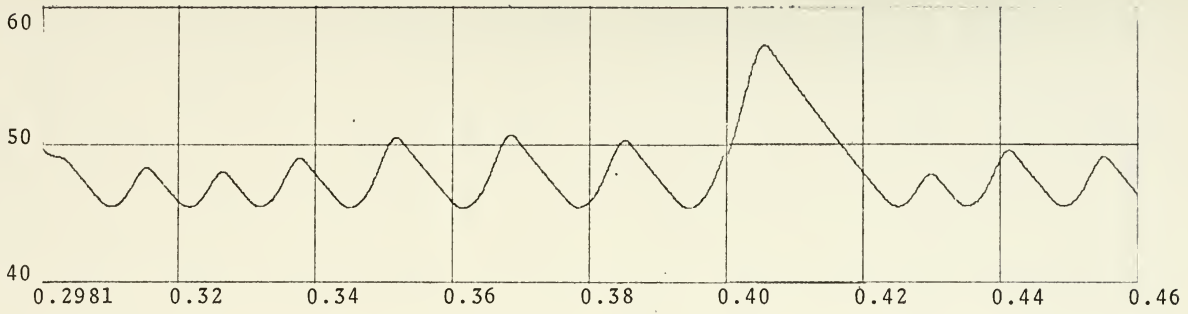

FIGURE 2.10a. Output waveform for R = 0.8Ω, V_{ref} = 46V.

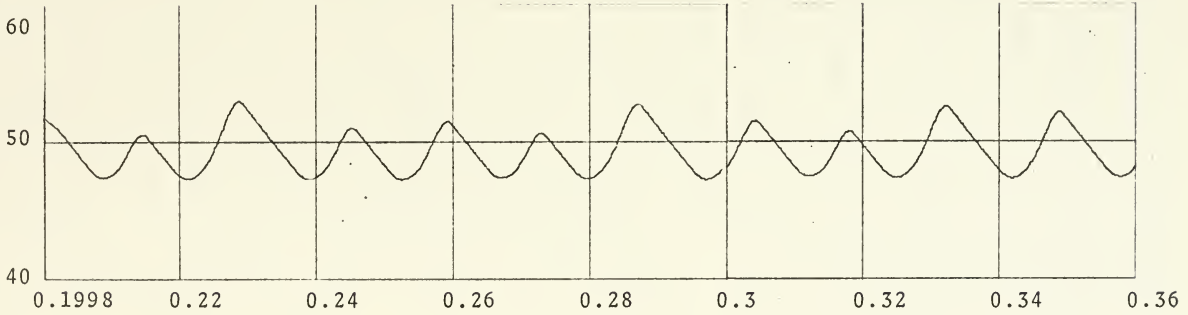

FIGURE 2.10b. Output waveform for R = 0.8Ω, V_{ref} = 48V.

III. INTRODUCTION TO THEORY OF SUBHARMONIC RESONSNCE

Subharmonic resonance is a phenomenon which occurs in nonlinear systems. Usually the nonlinear system subharmonic resonance frequency is a fraction of the input frequency. As an example consider the limit cycling voltage regulator system which is introduced in this thesis, or a relaxation oscillator, or a moving-coil loudspeaker with a non-uniform magnetic field are the common examples of the subharmonic resonance. This phenomenon can also occur in servo mechanisms with saturation or with other nonlinearities. In all of these cases the lowest frequency present at the output is a submultiple of the input frequency and usually at or near the natural frequency of the system. The system output amplitude would be different depending on the existence of the subharmonic. Such subharmonics can increase or decrease the output amplitude. For systems in which the output is intended to reproduce the input as closely as possible, as is the motion of the loudspeaker cone or a servo motor, this phenomenon can introduce an intolerable distortion. Also it is observed that in limit cycling voltage regulator systems, subharmonics can cause instability of the system. Also one of the important points, subharmonic resonance does not occur in pure linear systems. If subharmonics are not wanted the best way to eliminate them is by changing the parameters of the linear system or placing a compensation element rather than trying to change the nonlinear part of the system.

It is possible to predict subharmonic resonance in the nonlinear system by using the Dual input Describing function and by solution of the nonlinear differential equation. There are some disadvantages to the second method. Since the output of the nonlinear element is expressed as a power series of the input, successive approximations to the correct solution converge rapidly only if the amount of nonlinearity is small. And also the solution of the differential equation does not give a physical picture of the mechanism of subharmonic resonance.

Subharmonic resonance normally exists only in lightly damped systems with nonlinear energy delays or with nonlinear restoring forces. In systems giving rise to subharmonics, the nonlinear element is frequently characterized by hysteresis. Typical nonlinearities are backlash, magnetic hysteresis loops and relays, etc. It is also important to note that generation of subharmonics is dependent on initial conditions, i.e., they may occur in a certain range of amplitudes and frequencies. If in a system a subharmonic is obtained it stays "locked in" over a reasonable frequency range. If the driving frequency is changed to a new value, the system output frequency changes also to a new value which is ω/n, ω being the driving frequency and n order of subharmonic.

IV. DUAL INPUT DESCRIBING FUNCTION FOR PREDICTION OF SUBHARMONICS

In the voltage regulator system, power supply ripples feed around the loop and interact with the nonlinearity of the system and cause instability of the system. The limit cycle resulting from this instability is at a submultiple of the ripple frequency and is commonly called a subharmonic resonance. Normal describing function theory cannot predict the existence of the subharmonic resonance. But by using the Dual input describing function method, it is possible to find a mathematical description of the nonlinear part of the system which can be used to predict the existence of these resonances. In general the forward transfer function of the voltage regulator system can be written

$$\frac{Vout}{E} = N(j\omega).G(j\omega) \qquad (4\text{-}1)$$

and

$$N(j\omega) = N_o(j\omega)+N_1(j\omega)$$

in which N ($j\omega$) is the DIDF due to the DC input to the nonlinearity of the system and $N_1(j\omega)$ is due to AC input to the nonlinearity. $G(j\omega)$ is the transfer function of the linear part of the system. If E represents an input to the nonlinearity then equation (4-1) can be rewritten,

$$\frac{Vout}{E} = N_o.G(j\omega)+N_1.G(j\omega) \qquad (4\text{-}2)$$

Frequency analysis is accomplished in the usual fashion, by applying the Nyquist criterion. The result could be interpreted as an encirclement of the -1+jo point. Therefore, equation (4-2) can be drawn in vector form as shown in Figure 4.1. It is seen from Figure 4.1 that the $N_1.G(j\omega)$ vector is placed at the tip of the $N_o.G(j\omega)$ vector. Because $N_o(j\omega)$ represents the DC part of the DIDF and $N_1(j\omega)$ represents the AC part of the DIDF, $N_o(j\omega)$ will have one component but $N_1(j\omega)$ will have many components as the phase angle changes. But during this variation $\omega = \omega_x$ must be constant. Then if (for different ω_x) this vector plot is repeated Figure 4.2 would be obtained. The $N_1.G(j\omega)$ vector would be placed on the tip of the $N_oG(j\omega)$ as phase is varied. By following this procedure many curves can be drawn and if any of these curves $N_1.G(j\omega)$ encircles the -1+jo point then in Nyquist sense the system may be unstable. Such a system may have a subharmonic resonance, but this is not guaranteed.

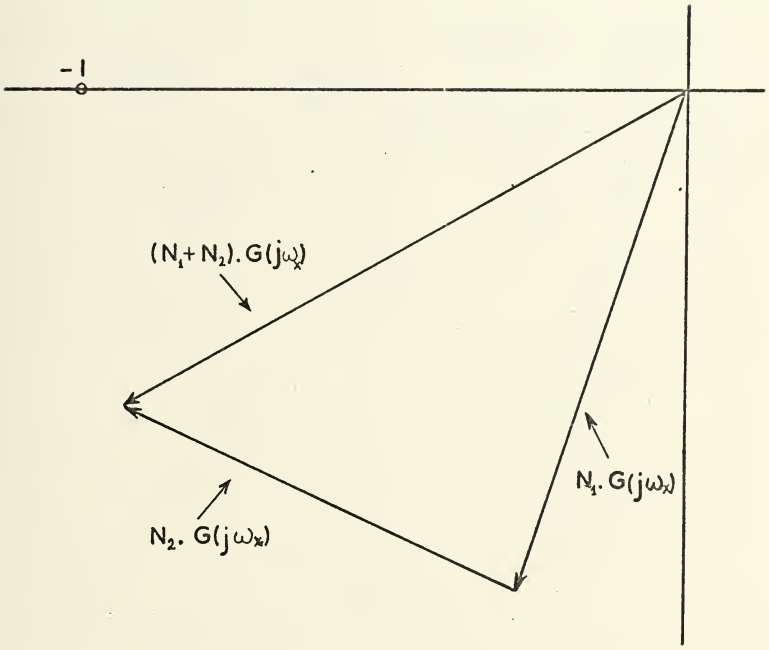

FIGURE 4.1. Vector diagram using DIDF.

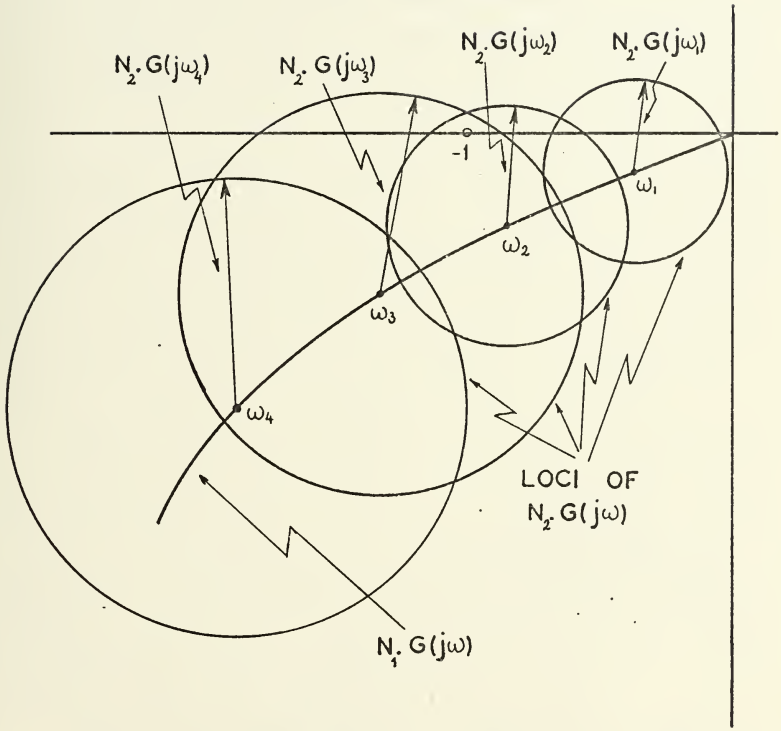

FIGURE 4.2. Analysis of the DIDF.

V. ANALYSIS OF THE EXPERIMENTAL RESULTS

A. ANALYSIS OF LIMIT CYCLING VOLTAGE REGULATOR

The goal is to find out the exact cause of subharmonics in the limit cycling voltage regulator system. For this purpose the IBM-360 computer was used for solving system differential equations and subroutine INTEG 2 is used. Appendix B shows this computer program and as an example one of the outputs. The output graph was obtained for three different loads and in each case V_{ref} is changed from 64 volt to 46 volt. Each run was permitted enough time so that the system reached steady state. From these output plots by analyzing the wave shape of the output, the results in Table 5-1, Table 5-2, and Table 5-3 were obtained.

Those tables showed that the system has mostly 1/2 order subharmonics and a few 1/4, 1/8 subharmonics. Then it may be said that the limit cycling voltage regulator system has an even order nonlinearity. Because most experimental results have shown that nonlinearities of even order give even order subharmonics.

In the Tables amplitudes are given peak to peak in volts. These amplitudes are given as the observed values of the output's highest spike and lowest spike. These lowest and highest spikes become smaller if the load resistance is increased. Increasing load resistance caused increase in the ripple instability at the output. For many cases it

ANALYSIS OF OUTPUTS FOR R=0.8 Ω

REFERENCE VOLTAGE V_{REF} (VOLT)	LARGER AMPLITUDE (PP. VOLT)	SMALLER AMPLITUDE (PP. VOLT)	LIMIT CYCLE FREQUENCY (Hz)	SUBHARMONIC FREQUENCY (Hz)	ORDER OF SUBHARMONIC
64	8.66	8.66	29.8	---	---
62	7.1	6.7	35.8	17.85	1/2
60	5.9	5.9	39.7	---	---
58	4.72	4.32	50.8	25.4	1/2
56	5.5	5.11	50.8	25.4	1/2
54	3.5	3.15	68.6	35.8	1/2
52	4.72	4.72	57.8	---	---
50	2.76	2.36	87.8	44.6	1/2
48	5.31	1.97	56.2	28.1	1/2
46	11.8	1.77	68.4	17.1	1/4

TABLE 5-1

ANALYSIS OF OUPUTS FOR R=1.6 Ω

REFERENCE VOLTAGE V_{REF} (VOLT)	LARGER AMPLITUDE (PP. VOLT)	SMALLER AMPLITUDE (PP. VOLT)	LIMIT CYCLE FREQUENCY (Hz)	SUBHARMONIC FREQUENCY (Hz)	ORDER OF SUBHARMONIC
64	5.3	5.7	27.8	13.35	1/2
62	3.54	3.54	35.8	---	---
60	1.97	1.77	57.8	28.7	1/2
58	1.18	1.18	134.0	---	---
56	0.985	0.985	115.5	---	---
54	2.76	0.788	115.0	25.4	1/4
* 52	3.15	0.984	145.6	72.8	1/2
50	3.15	0.59	57.8	25.4	1/2
* 48	3.55	1.22	73.68	3.21	1/8
* 46	4.32	1.37	80.8	40.4	1/2

* Subharmonic is determined by Fourier analysis.

TABLE 5-2

ANALYSIS OF OUTPUTS FOR R=3.2 Ω

REFERENCE VOLTAGE V_{REF} (VOLT)	LARGER AMPLITUDE (PP.VOLT)	SMALLER AMPLITUDE (PP.VOLT)	LIMIT CYCLE FREQUENCY (Hz)	SUBHARMONIC FREQUENCY (Hz)	ORDER OF SUBHARMONIC
64	3.15	3.15	21.2	---	---
62	1.57	1.48	39.7	19.85	1/2
60	1.18	0.788	68.8	36.2	1/2
* 58	2.36	0.394	104.8	52.4	1/2
56	1.575	0.985	90.6	25.5	1/2
* 54	1.77	0.59	100.0	50.0	1/2
52	1.575	0.786	91	23	1/4
* 50	5.9	0.394	63.6	17.4	1/4
* 48	2.75	1.18	62.88	31.44	1/2
* 46	3.94	0.53	49.28	12.32	1/4

*Subharmonic is determined by Fourier analysis.

TABLE 5-3

was not possible to determine the order of the subharmonics by inspection of the output curves. In these cases a Fourier analysis was made to establish the subharmonic frequencies and amplitudes.

Figure 5.1a to 5.1d shows the wave form at the filter element and from Figure 5.2 to Figure 5.34 shows the output and input plot to the filter. If one of the input plots is carefully observed one notices the difference in width of these pulses. The system has sinusoidal input to the thyristors and the output of this rectifier goes to the filter. This will charge the capacitor at the filter and when the output reaches V_{ref} the relay would be open but at this moment the rectifier will still continue to conduct and during these times the capacitor will charge. Afterwards it will discharge till the output voltage reaches V_{ref}. If the output voltage is much higher than V_{ref} then the capacitor will discharge for a longer time, therefore, the system would give a different pulse width due to this effect. This can be seen by the different number of ripples at the top of the input voltage wave form.

Output plots from Figure 5.2 to Figure 5.11 are for load resistance R = 3.2Ω. At lower voltages deciding the order of the subharmonic by inspection becomes impossible. Those outputs were analyzed in Fourier point of view and those outputs obtained by using Fourier analysis are designated with asterisks in the Table.

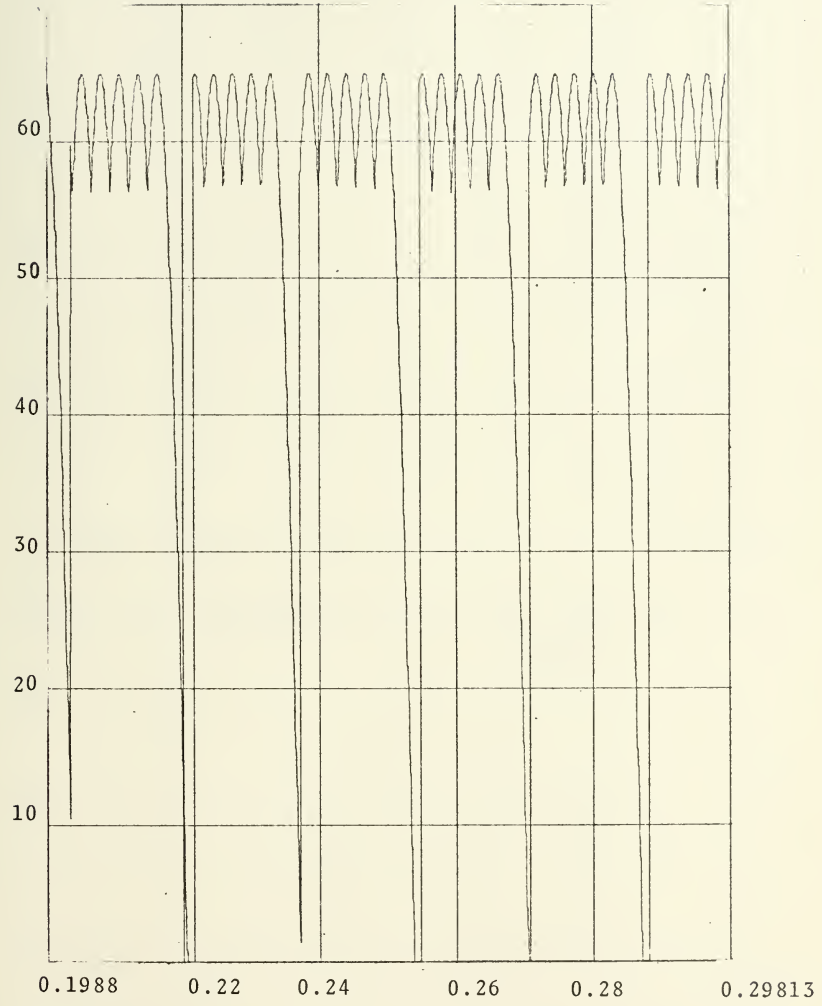

FIGURE 5.1a. Input to the filter, V_{ref} = 60, R = 1.6Ω

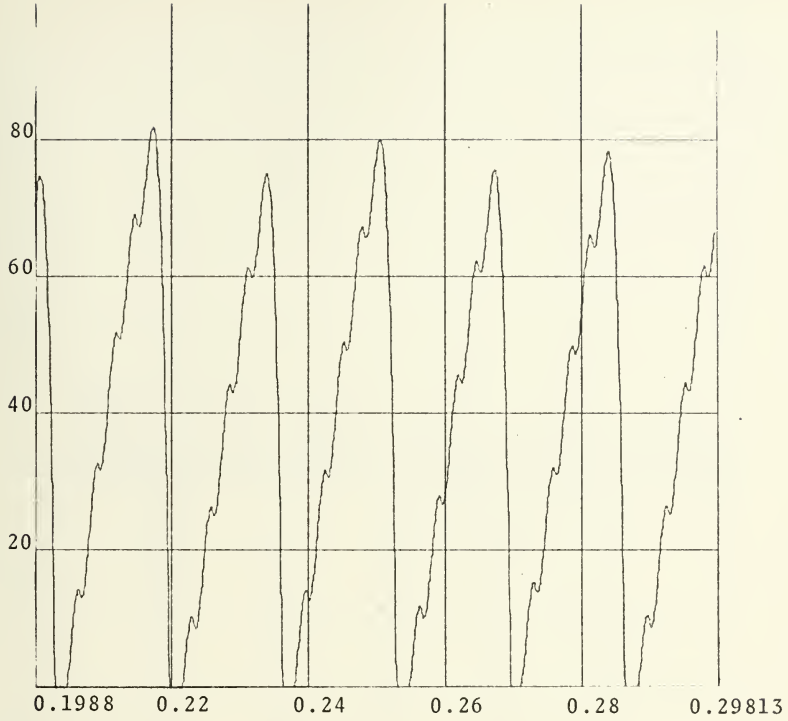

FIGURE 5.1b. Inductance current, V_{ref} = 60V., R = 1.6Ω

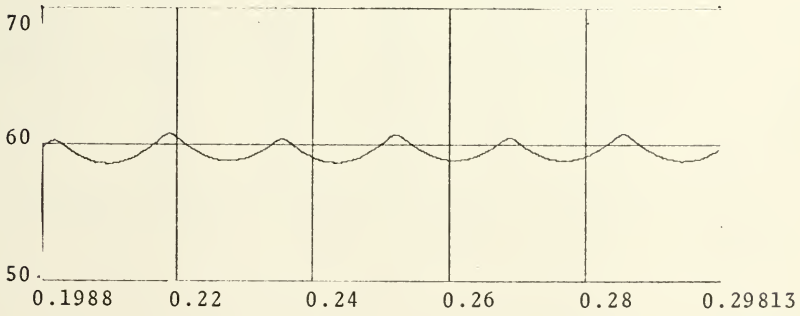

FIGURE 5.1c. Output voltage, V_{ref} = 60V., R = 1.6Ω

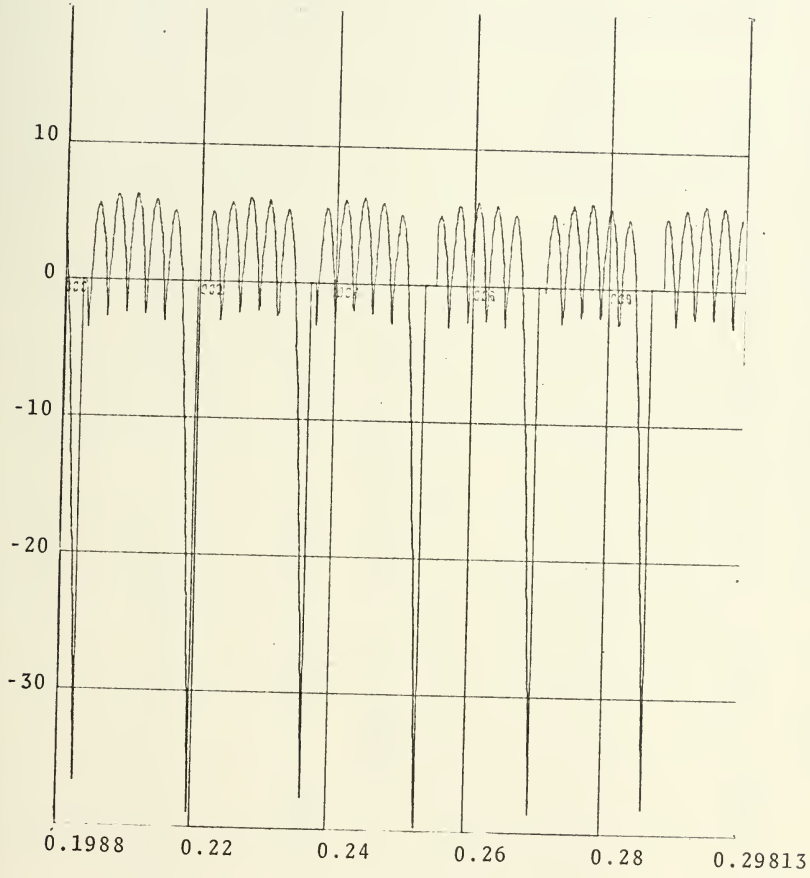

FIGURE 5.1d. Inductance voltage for V_{ref} = 60V., R = 1.6Ω

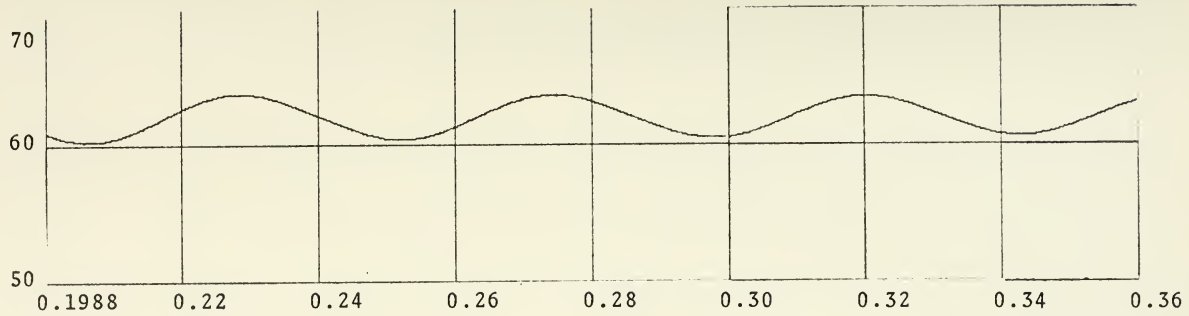

FIGURE 5.2. Output voltage, V_{ref} = 64V., R = 3.2Ω

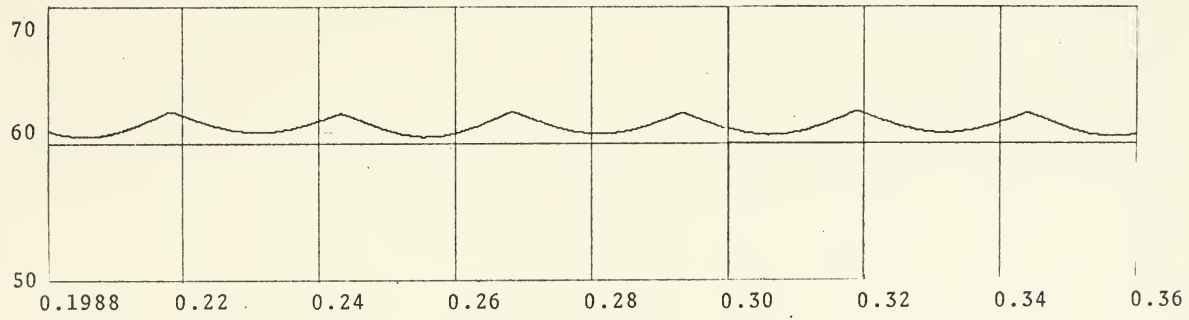

FIGURE 5.3. Output voltage, V_{ref} = 62V., R = 3.2Ω

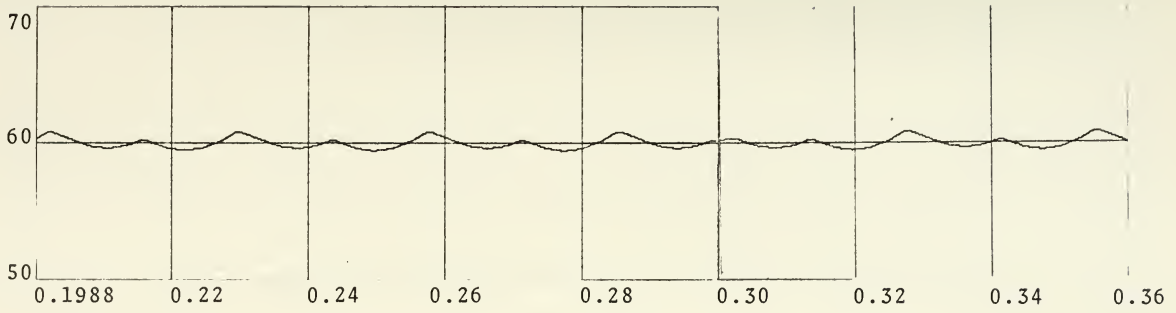

FIGURE 5.4. Output voltage, V_{ref} = 60V., R = 3.2Ω

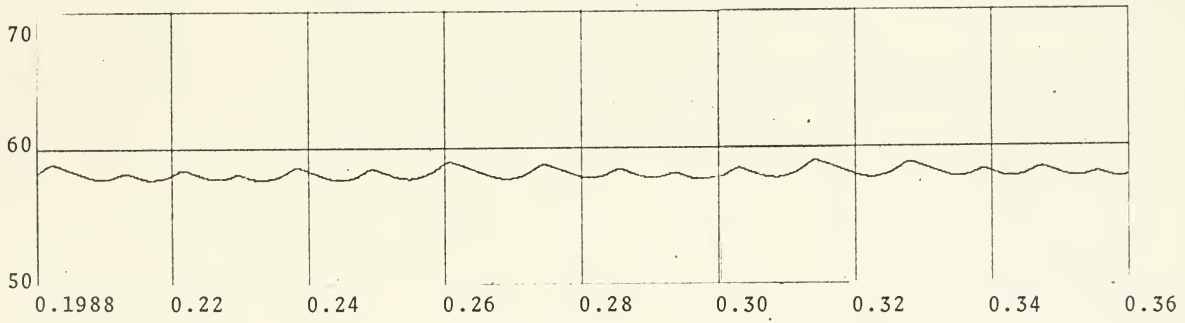

FIGURE 5.5. Output voltage, V_{ref} = 58V., R = 3.2Ω

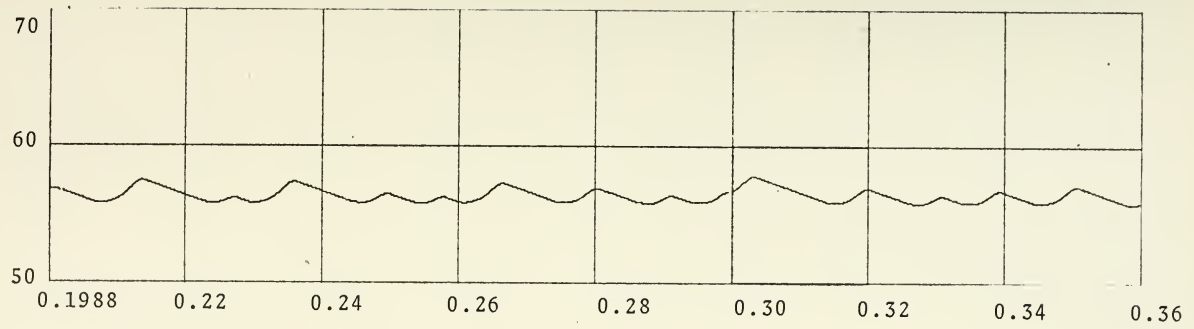

FIGURE 5.6. Output voltage, V_{ref} = 56V., R = 3.2Ω

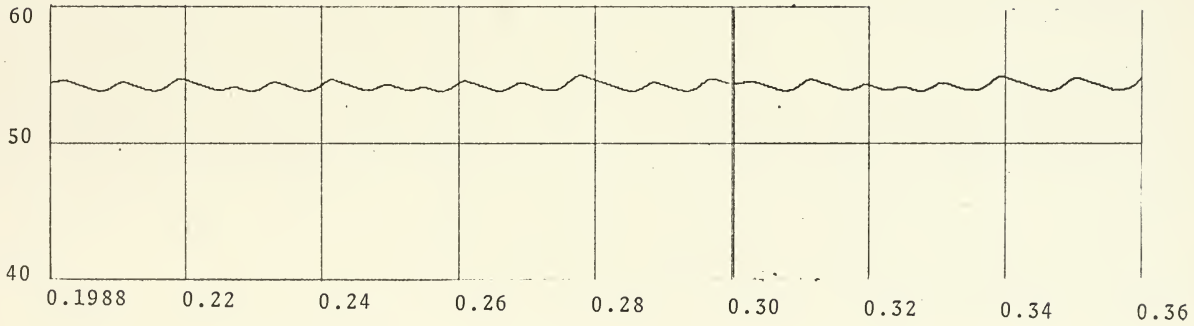

FIGURE 5.7. Output voltage, V_{ref} = 54V., R = 3.2Ω

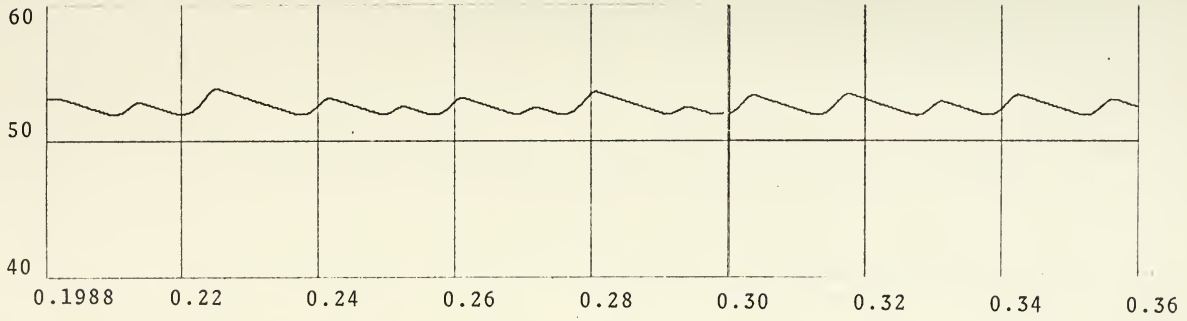

FIGURE 5.8. Output voltage, V_{ref} = 52V., R = 3.2Ω

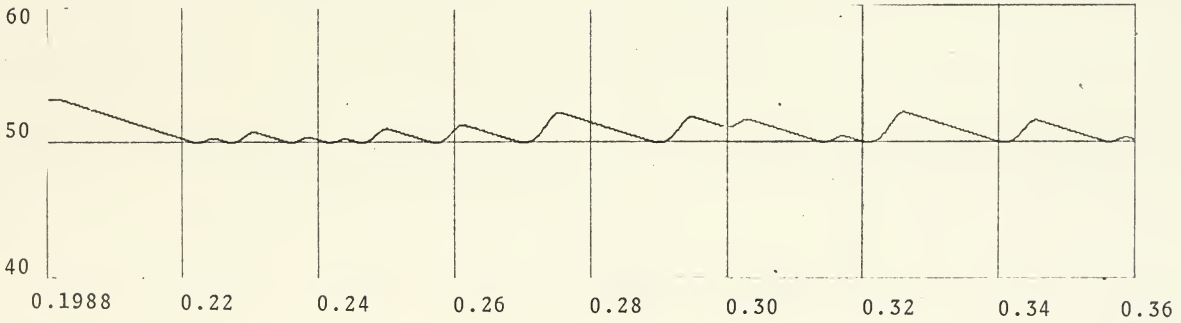

FIGURE 5.9. Output voltage, V_{ref} = 50V., R = 3.2Ω

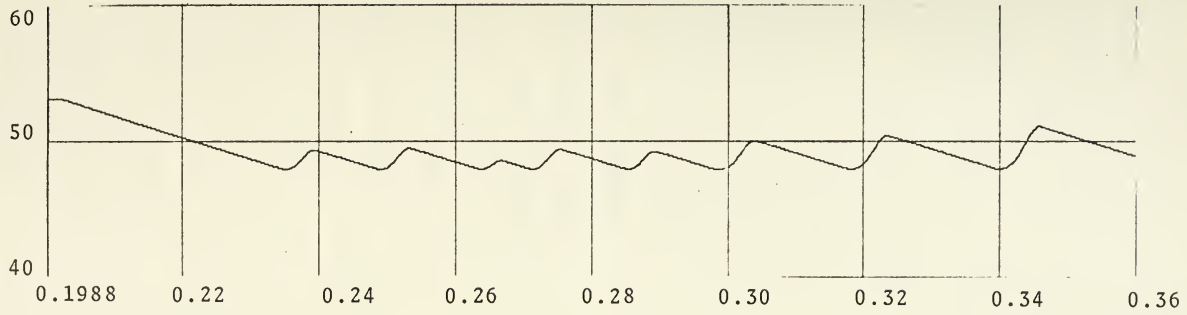

FIGURE 5.10. Output voltage, V_{ref} = 48V., R = 3.2Ω

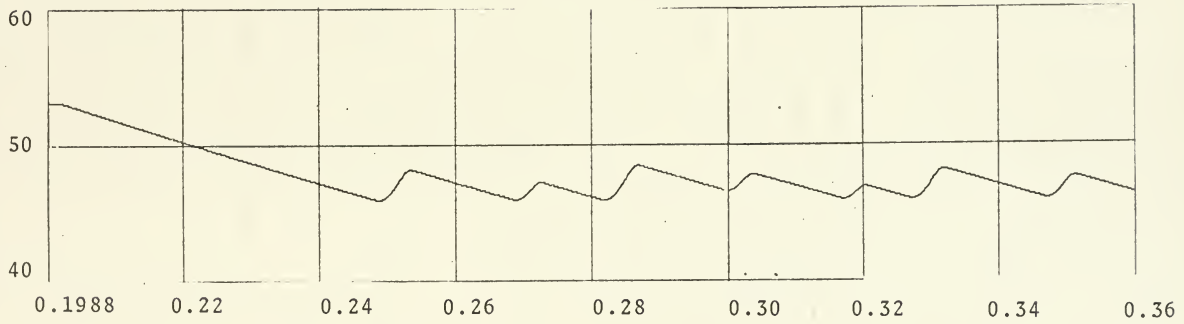

FIGURE 5.11. Output voltage, V_{ref} = 46V., R = 3.2Ω

Figure 5.12 to Figure 5.14 shows the input plot to the filter with average value of the pulse width approximately corresponding to the limit cycle frequency.

Output and input plot for the R = 1.6Ω case are shown in Figure 5.15 to Figure 5.26. For R = 0.8Ω case they are shown in Figure 5.27 to Figure 5.34.

B. ANALYSIS OF THE D-C SYSTEM

In this paper, one of the important things to be determined (if possible) is the exact cause of the subharmonics. Therefore, to get results it is necessary to make some change in voltage regulator system. Then it will be easy to see the effect of the element, (i.e., relay, thyristor). For this purpose the rectifier part was replaced with a D-C source, and the system was as shown in Figure 5.35.

For analysis of the system the C_i.5000 analog computer was used and the system output obtained for R = 0.8Ω, R = 1.6Ω, and R = 3.2Ω. In this system the filter unit was the same as for all other tests, the only change was replacing the rectifier with a 65 volt battery. Figure 5.36 shows the analog diagram for the C_i5000. Output and input plots for different loads are shown in Figure 5.37 to 5.39. These outputs show that the system did not have subharmonics. Also these runs were made for different V_{ref} conditions but the system never produced subharmonics. This means that if the system has a nonlinear element but does not have a periodic forced input then the system never gives subharmonics at the output. In order to have

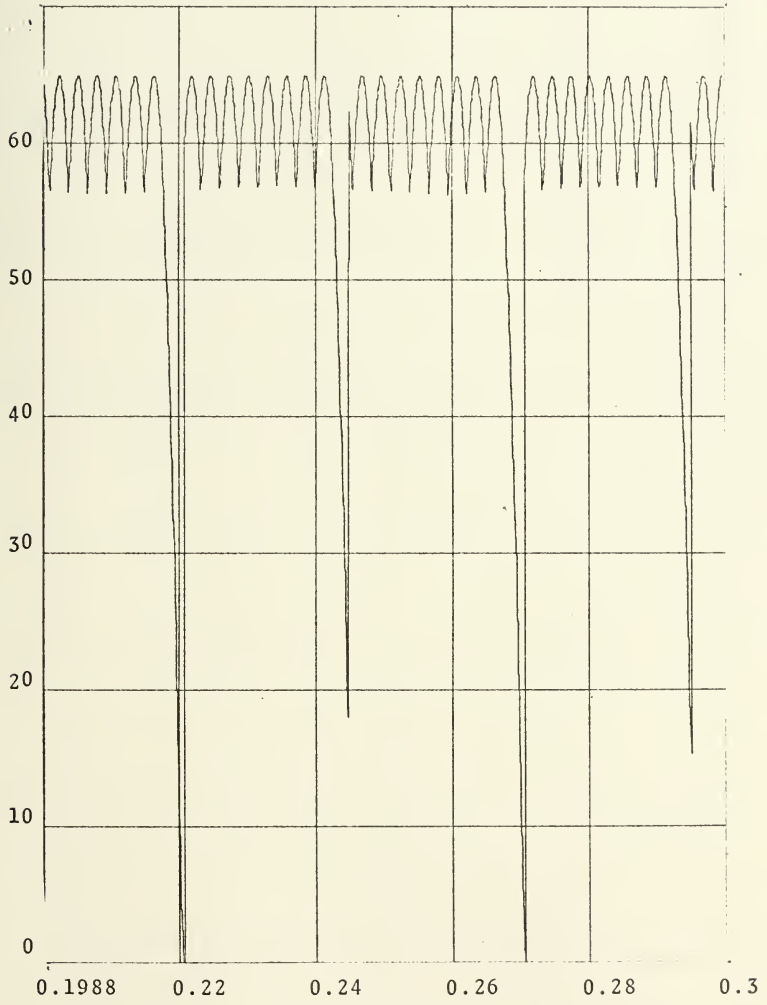

FIGURE 5.12. Voltage into the filter, V_{ref} = 62V, R = 3.2Ω

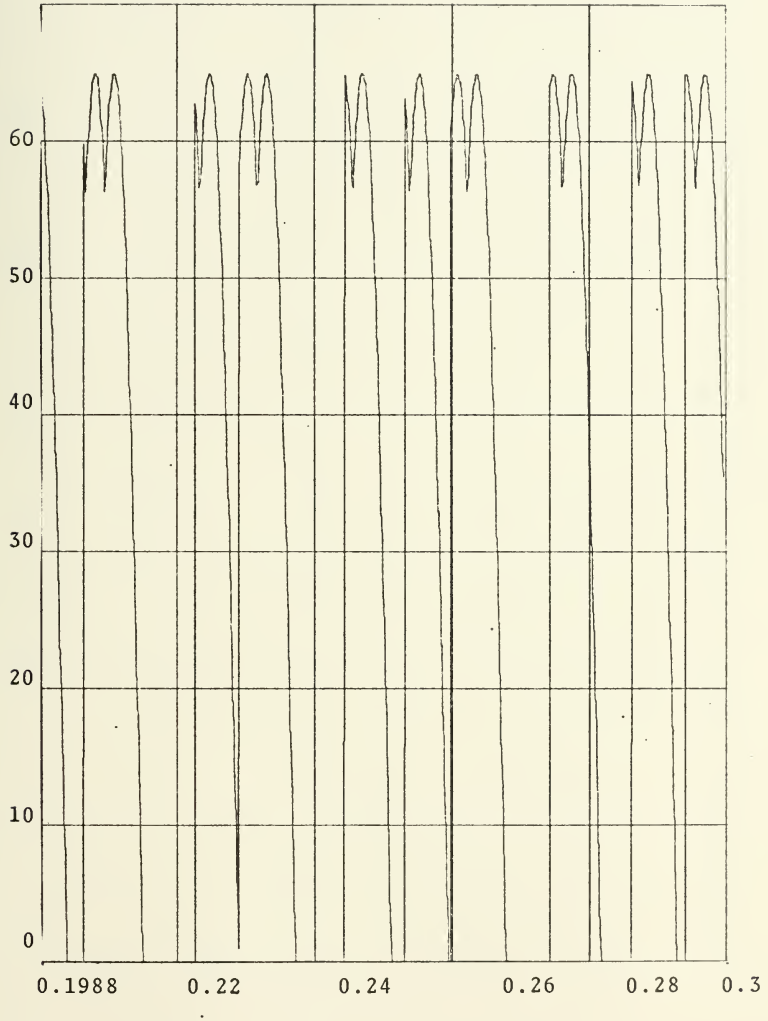

FIGURE 5.13. Voltage into the filter. V_{ref} = 56V., R = 3.2Ω

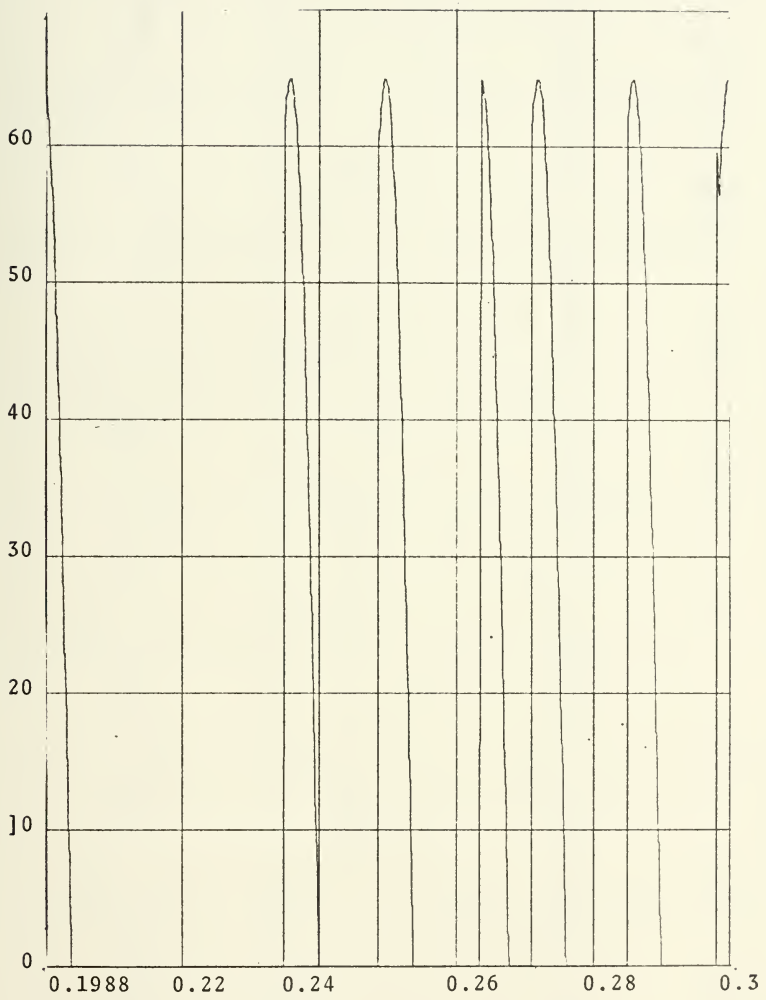

FIGURE 5.14. Voltage into filter, V_{ref} = 48V., R = 3.2Ω

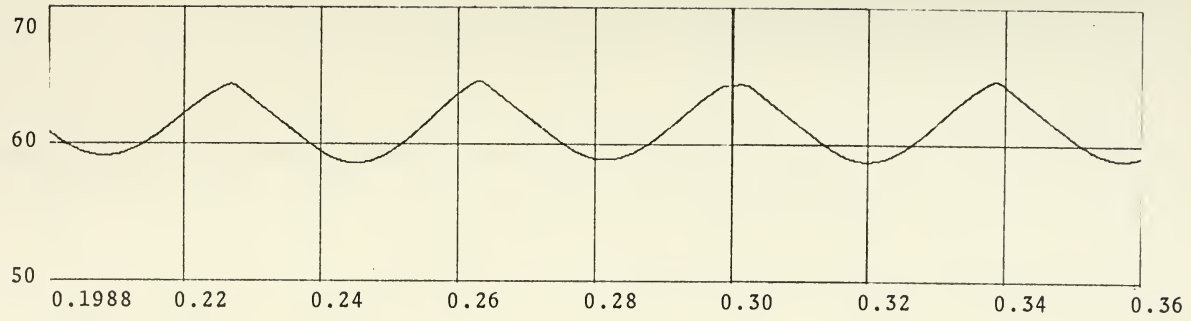

FIGURE 5.15. Output voltage, V_{ref} = 64V., R = 1.6Ω

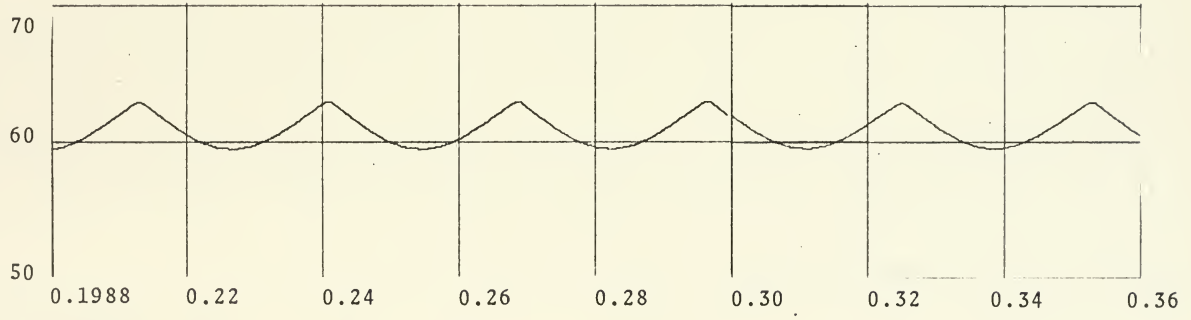

FIGURE 5.16. Output voltage, V_{ref} = 62V., R = 1.6Ω

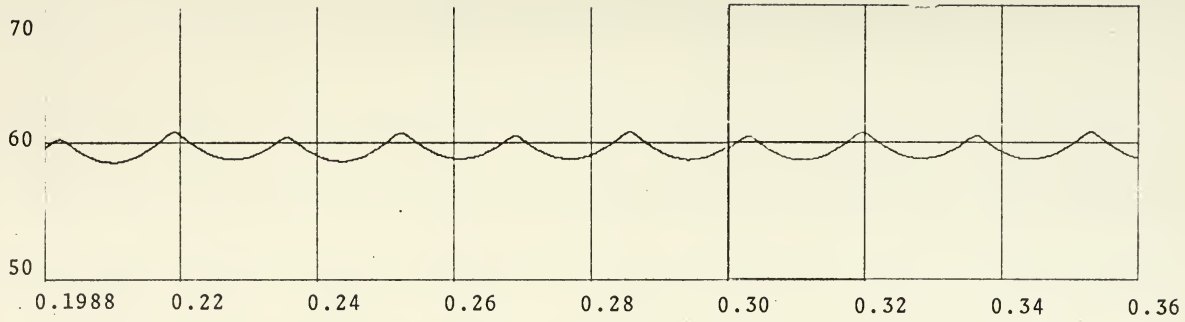

FIGURE 5.17. Output voltage, V_{ref} = 60V., R = 1.6Ω

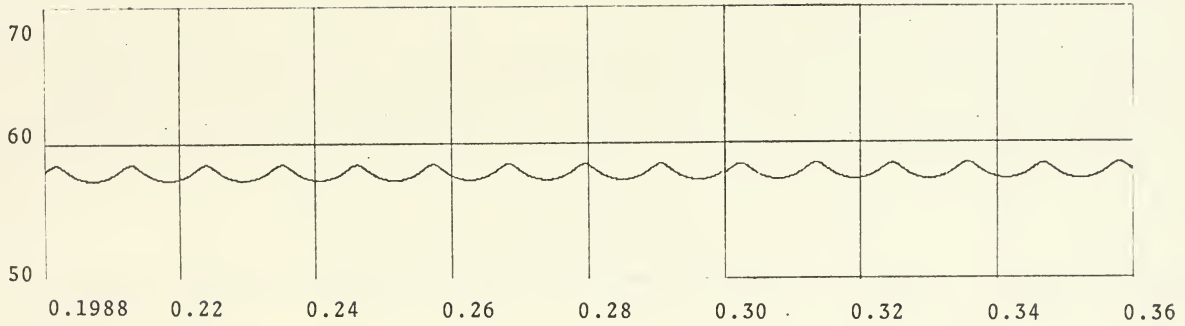

FIGURE 5.18. Output voltage, V_{ref} = 58V., R = 1.6Ω

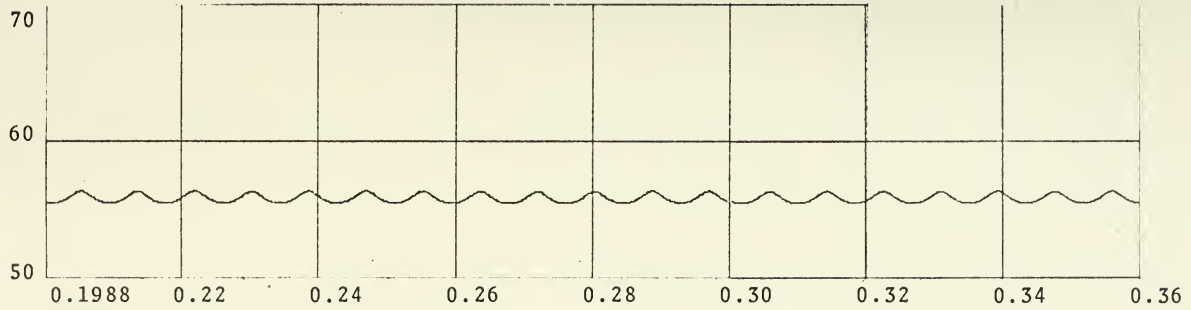

FIGURE 5.19. Output voltage, V_{ref} = 56V., R = 1.6Ω

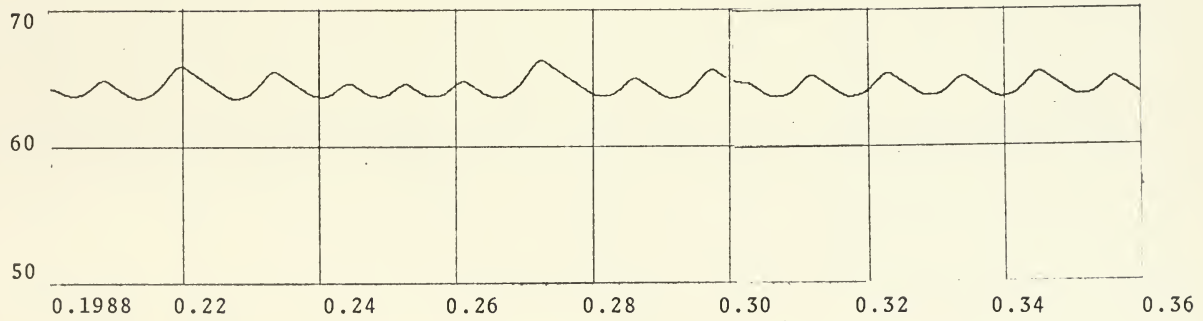

FIGURE 5.20. Output voltage, V_{ref} = 54V., R = 1.6Ω

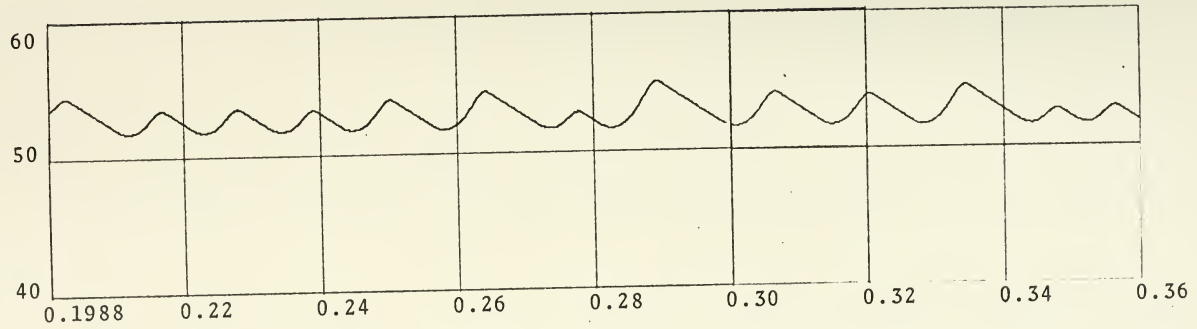

FIGURE 5.21. Output voltage, V_{ref} = 52V., R = 1.6Ω

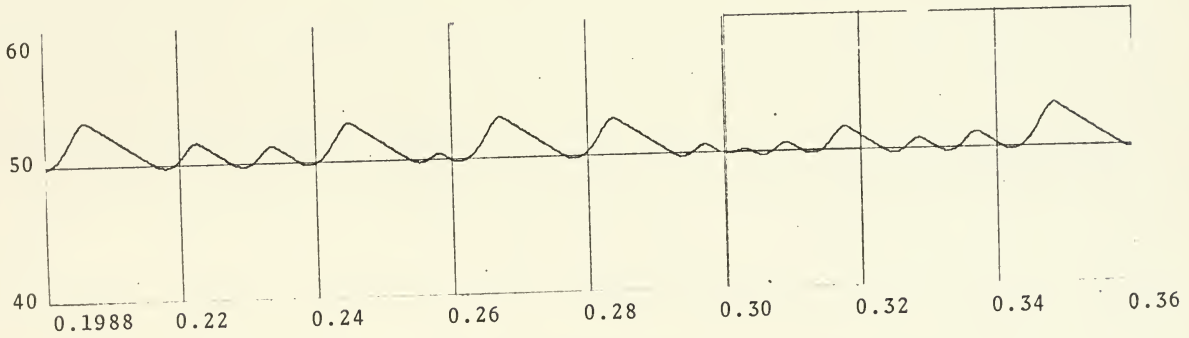

FIGURE 5.22. Output voltage, V_{ref} = 50V., R = 1.6Ω

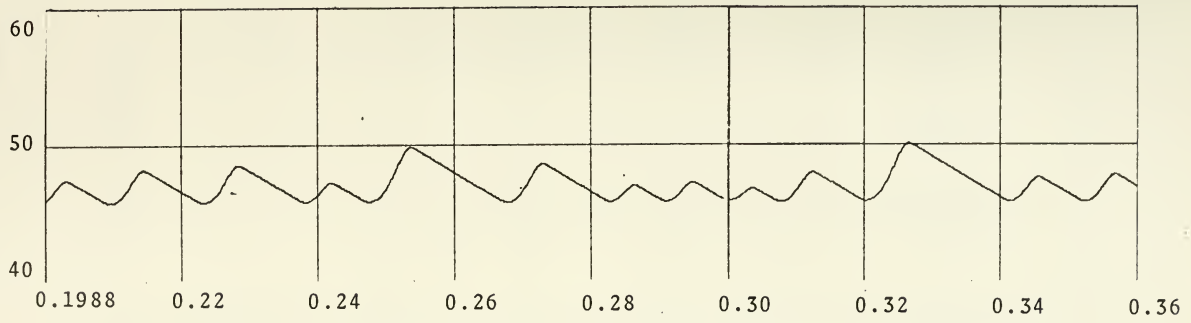

FIGURE 5.23. Output voltage, V_{ref} = 46V., R = 1.6Ω

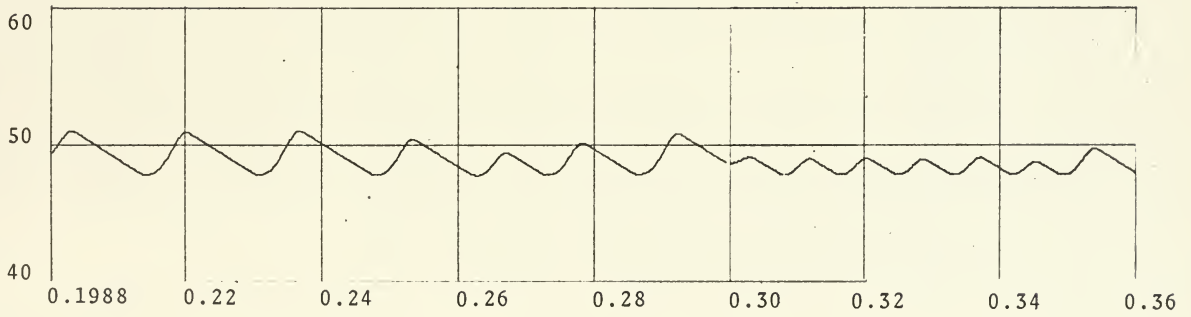

FIGURE 5.24. Output voltage, V_{ref} = 48V., R = 1.6Ω

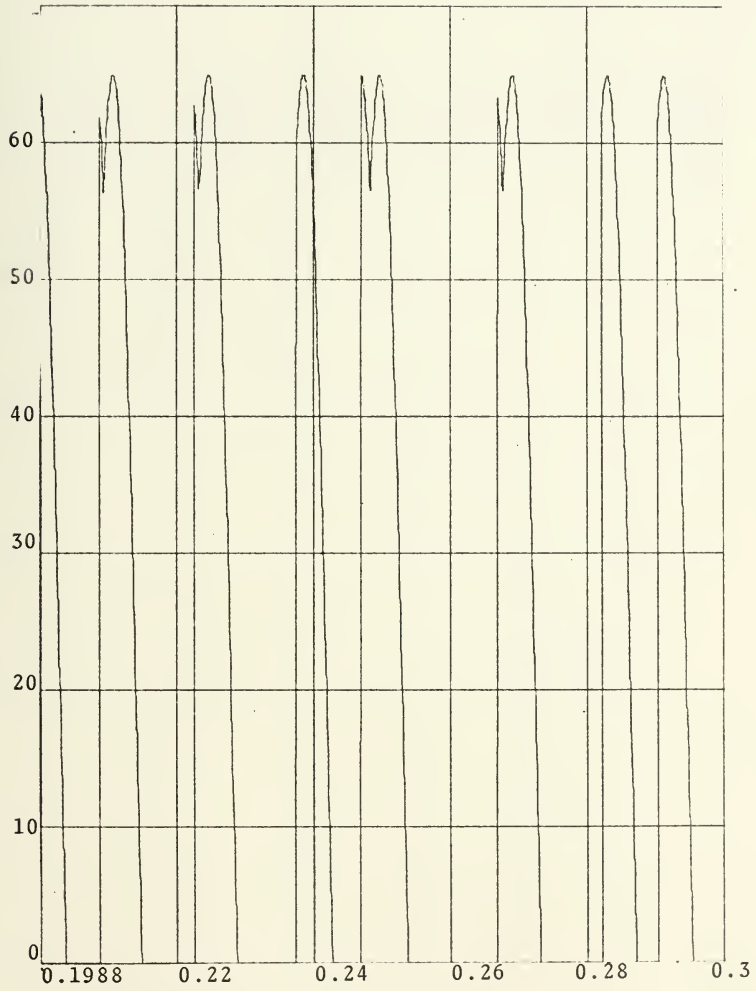

FIGURE 5.25. Voltage into filter, V_{ref} = 46V., R = 1.6Ω

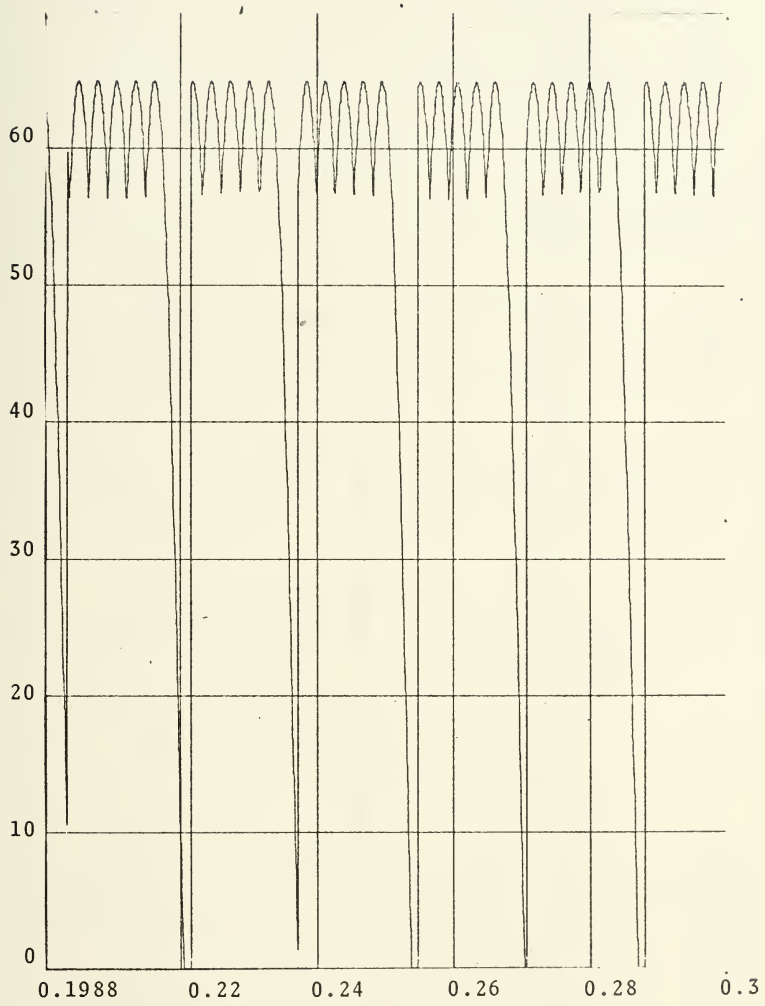

FIGURE 5.26. Voltage into filter, V_{ref} = 60V., R = 1.6Ω

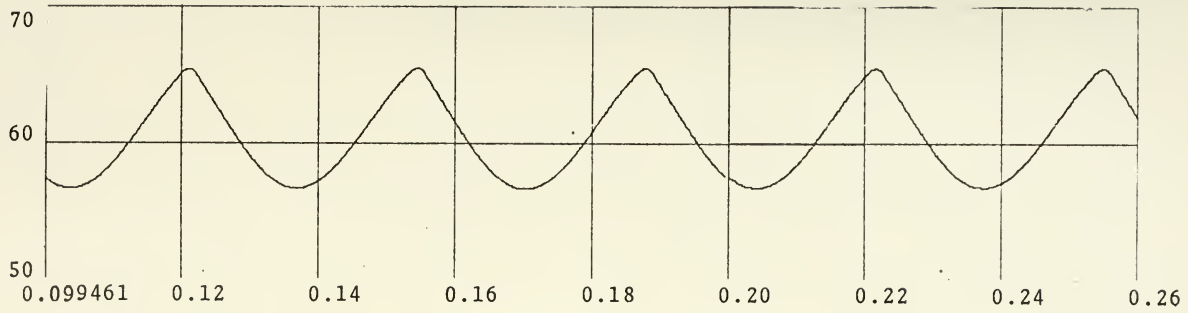

FIGURE 5.27. Output voltage, V_{ref} = 64V., R = 0.8Ω

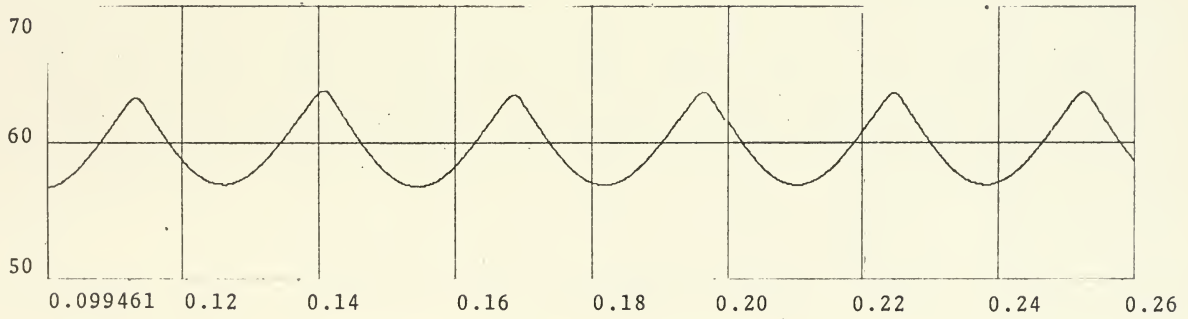

FIGURE 5.28. Output voltage, V_{ref} = 62V., R = 0.8Ω

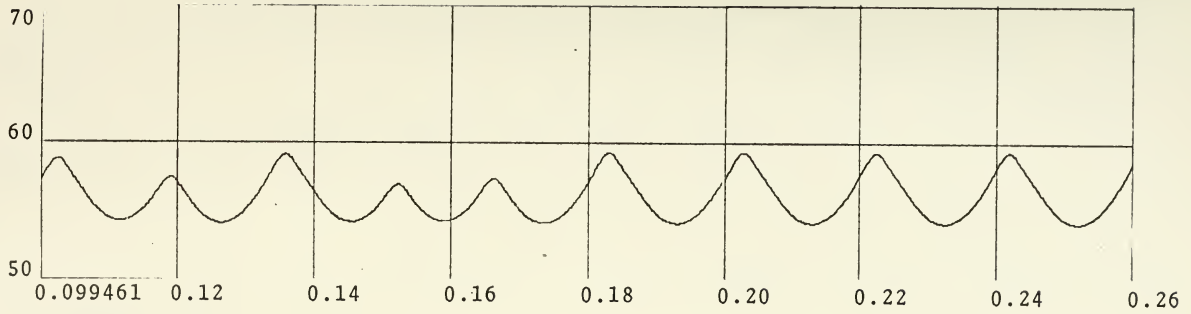

FIGURE 5.29. Output voltage, V_{ref} = 56V., R = 0.8Ω

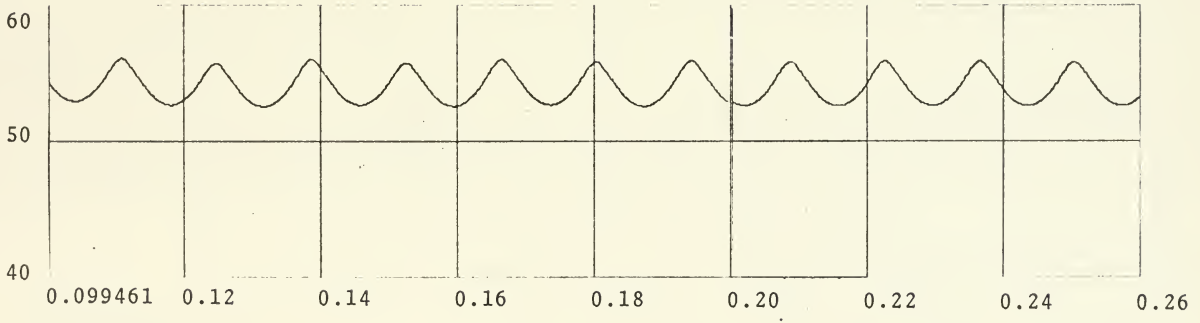

FIGURE 5.30. Output voltage, V_{ref} = 54V., R = 0.8Ω

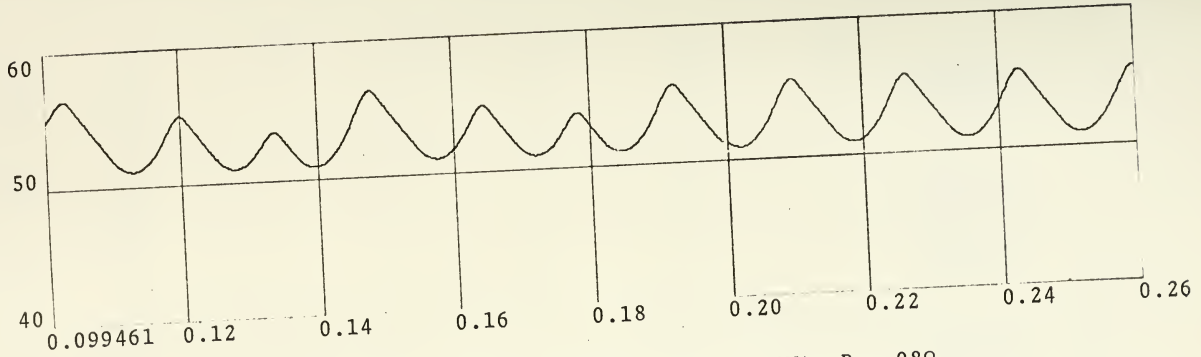

FIGURE 5.31. Output voltage, V_{ref} = 52V., R = 08Ω

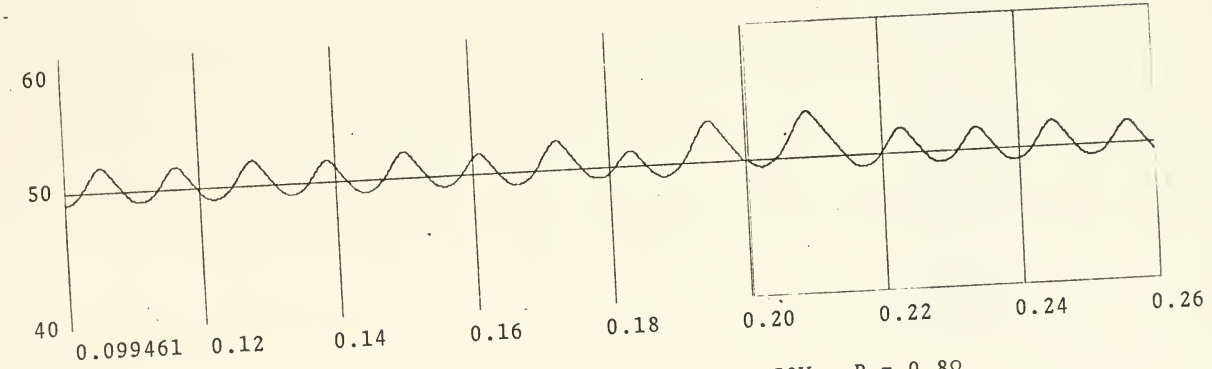

FIGURE 5.32. Output voltage, V_{ref} = 50V., R = 0.8Ω

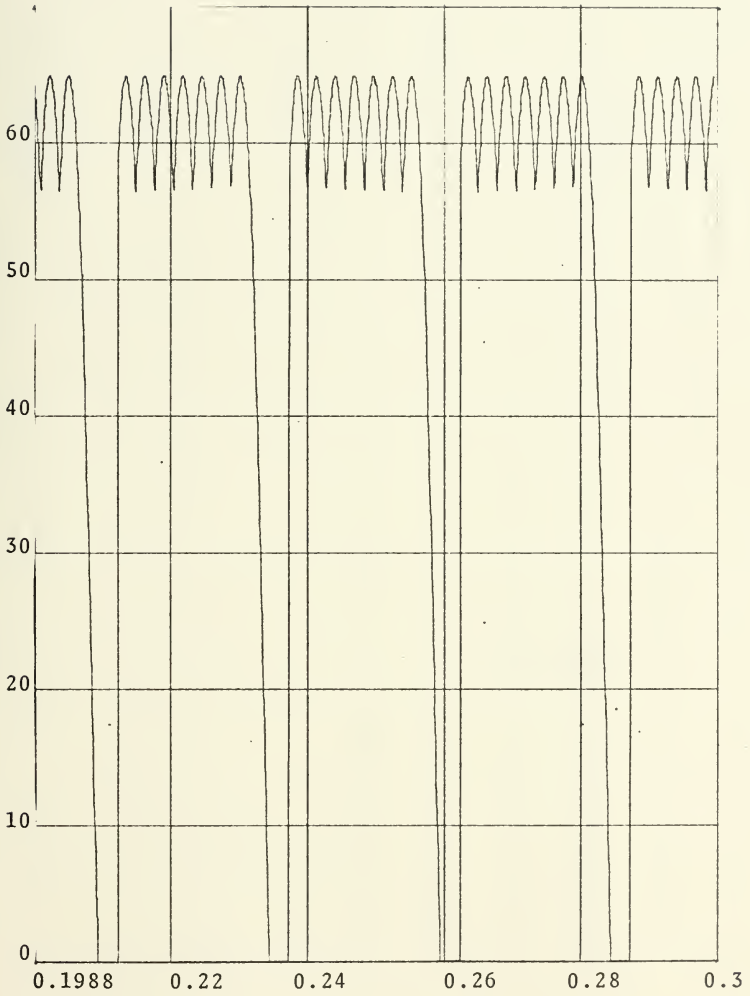

FIGURE 5.33. Voltage into filter, V_{ref} = 60V., R = 0.8Ω

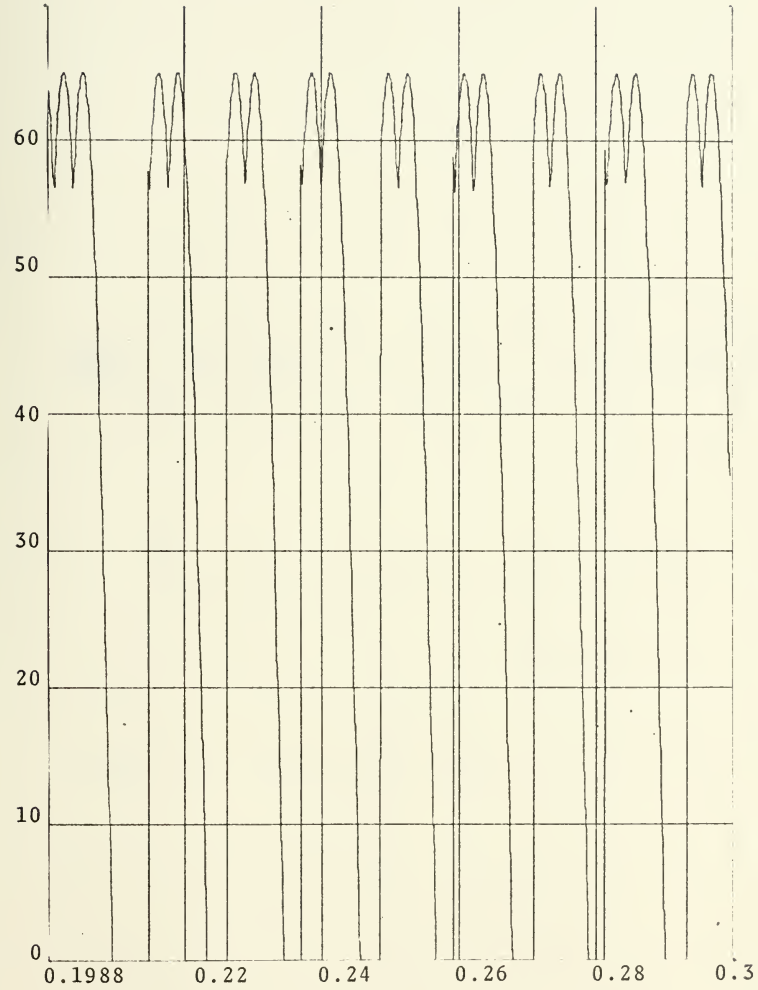

FIGURE 5.34. Voltage into filter, V_{ref} = 50V., R = 0.8Ω

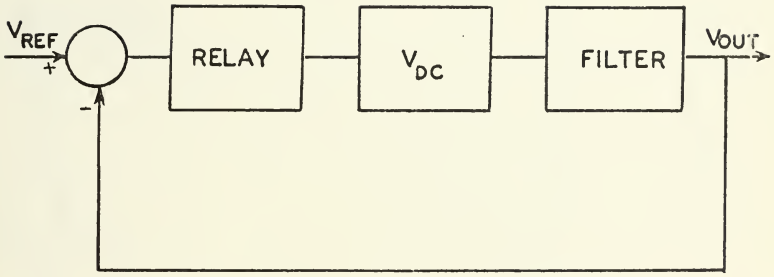

FIGURE 5.35. Basic block diagram of D-C case.

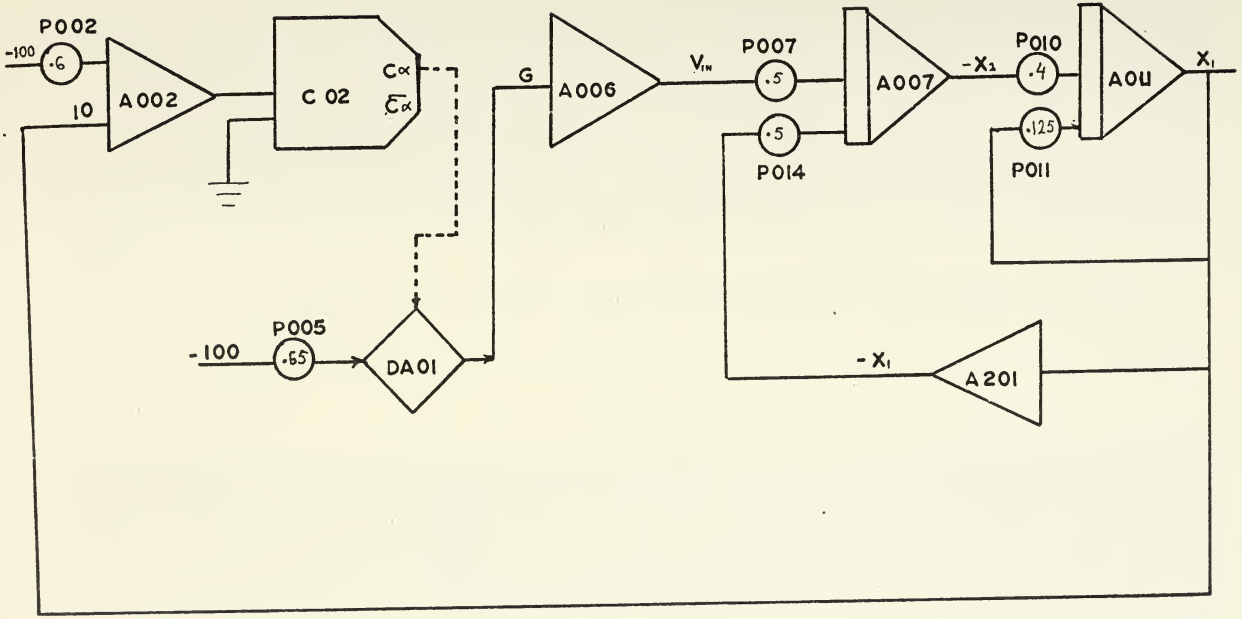

FIGURE 5.36. Analog diagram of D-C case.

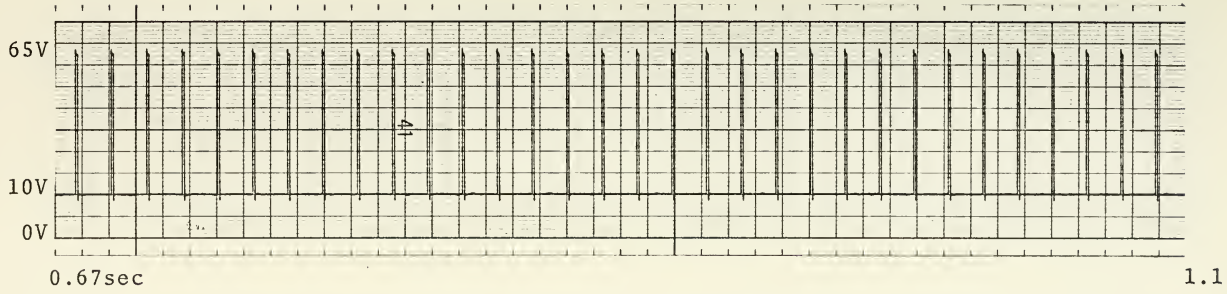

FIGURE 5.37a. Input voltage to the filter, V_{ref} = 62V, R = 0.8Ω

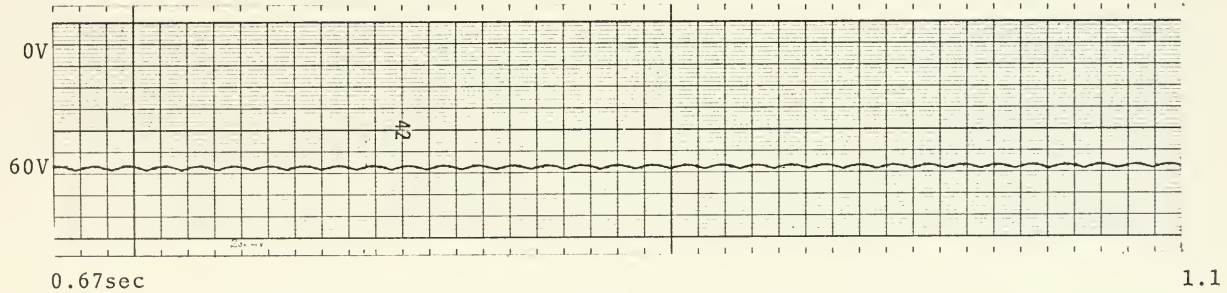

FIGURE 5.37b. Output voltage, V_{ref} = 62V., R = 0.8Ω

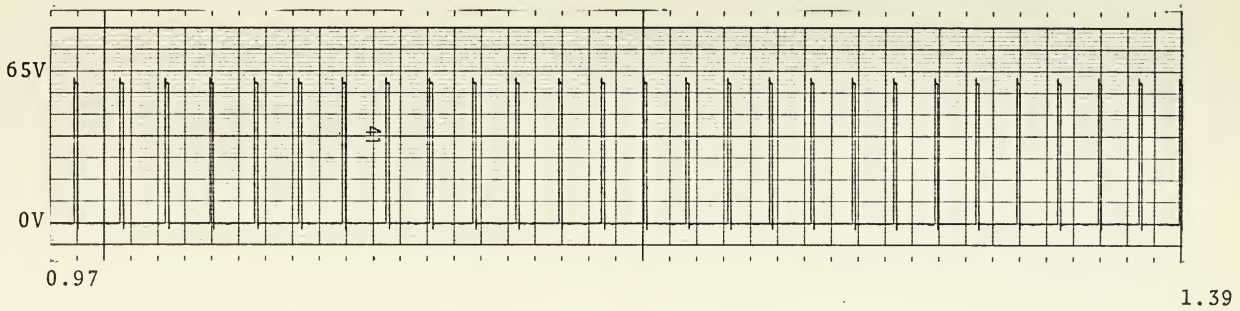

FIGURE 5.38a. Input voltage to the filter, V_{ref} = 62V., R = 1.6Ω

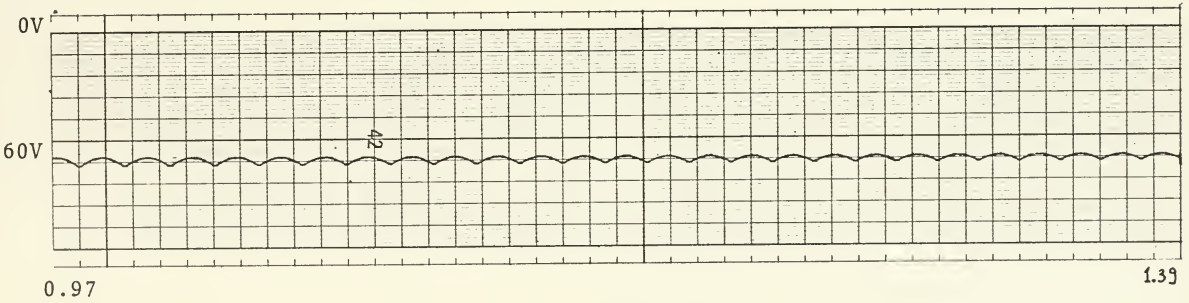

FIGURE 5.38b. Output voltage, V_{ref} = 62V., R = 1.6Ω

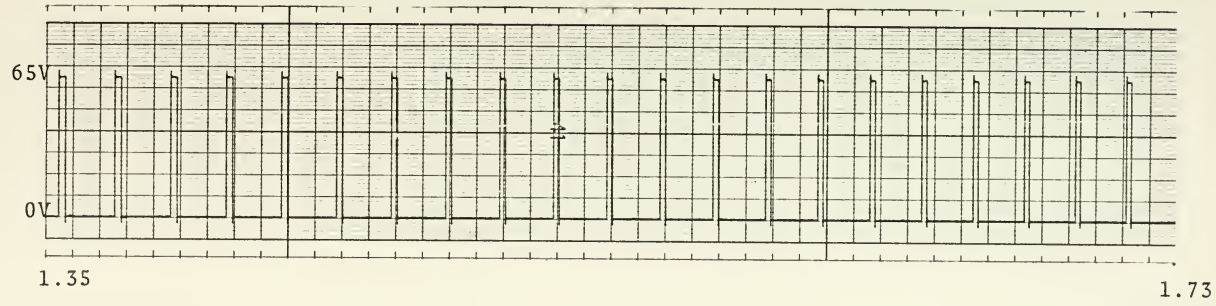

FIGURE 5.39a. Input voltage to the filter, V_{ref} = 62V., R = 3.2Ω

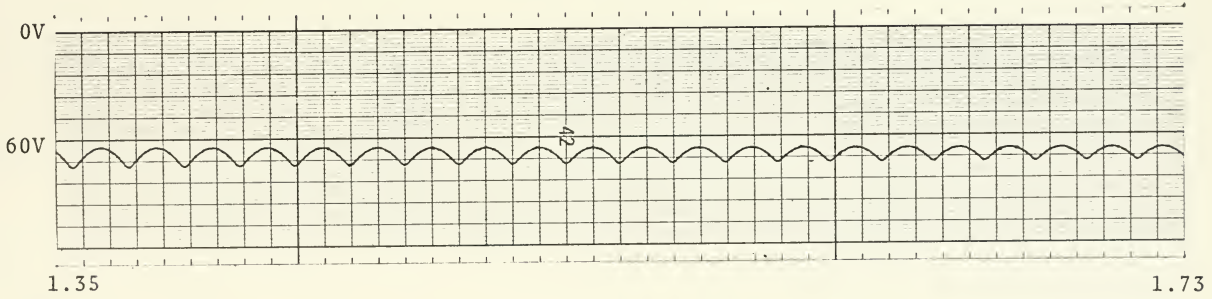

FIGURE 5.39b. Output voltage, V_{ref} = 62V., R = 3.2Ω

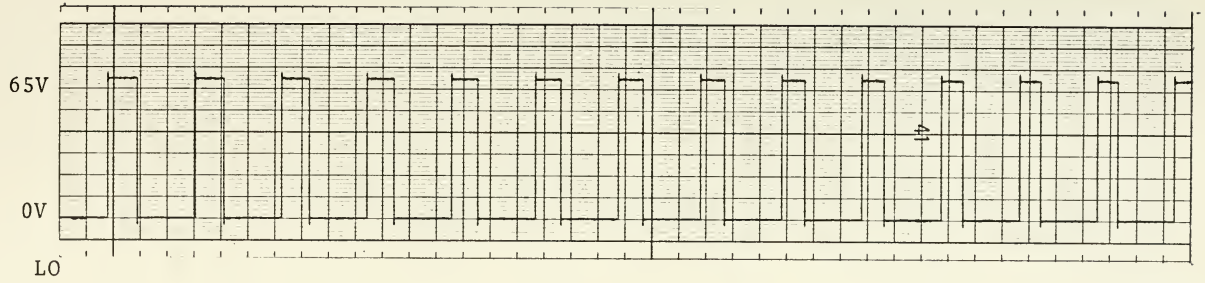

FIGURE 5.40a. Input voltage to the filter, V_{ref} = 62V., R = 3.2Ω

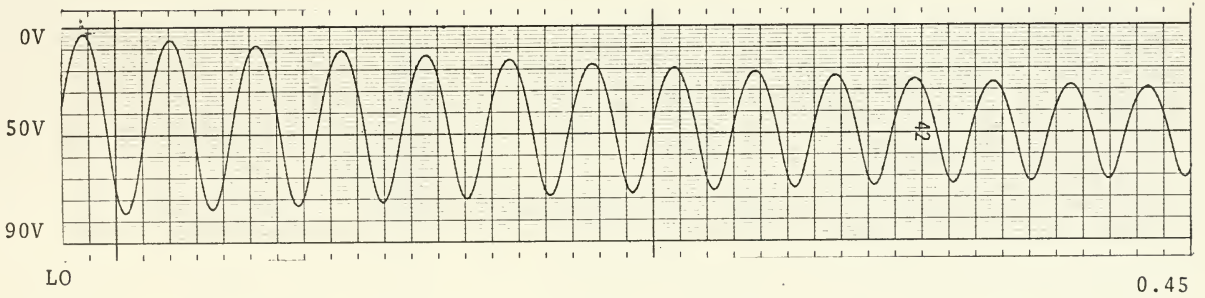

FIGURE 5.40b. Output voltage, V_{ref} = 62V., R = 3.2Ω

subharmonics, a control system must satisfy two conditions, i.e., the system must have a periodic input forcing function and a nonlinear element. From this it might be said that the exact cause of subharmonic in the limit cycling voltage regulator is due to the nonlinear part together with relay and rectifier and also the periodic input to the system from the AC ripple. It is important to remember that in order to have subharmonics the system usually must be lightly damped.

The block diagram shown for D-C case at Figure 5.36's detail of the elements are explained in Appendix C. The output and input plot of system shown from Figure 5.37 to Figure 5.39 are for steady state conditions. Figure 5.40 shows the change in pulse duration of the relay upon the system reaching the steady state.

C. GAIN CONSIDERATION

As a last investigation of the limit cycling voltage regulator, the gain was changed from 1 to 10,000 and the output plot was obtained for different values of gain. Figure 5.41, Figure 5.42, and Figure 5.43 show these output plots. Output shows that change in system gain did not effect the output wave form and it did not effect the subharmonic resonance.

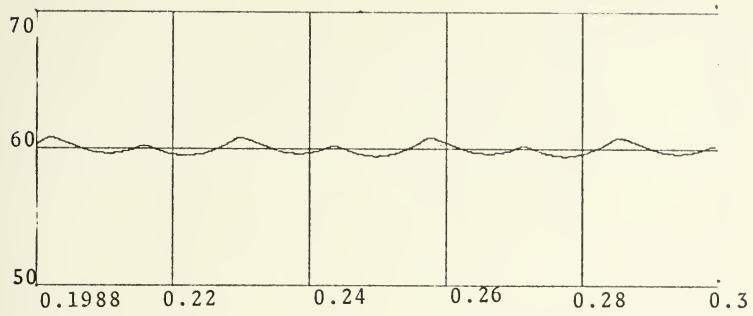

FIGURE 5.41a. Output plot, V_{ref} = 60V., R = 3.2Ω, Gain = 5.0

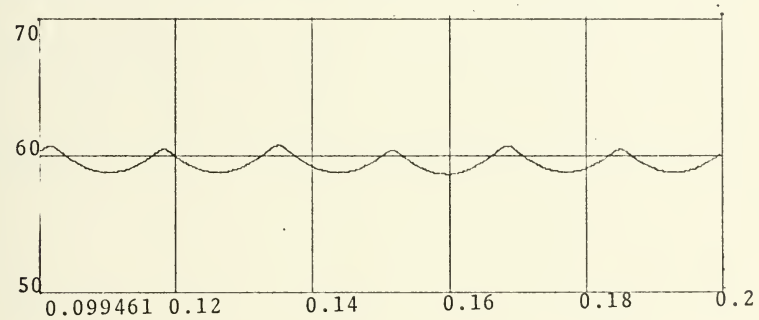

FIGURE 4.41b. Output plot, V_{ref} = 60V., R = 1.6Ω, Gain = 5.0

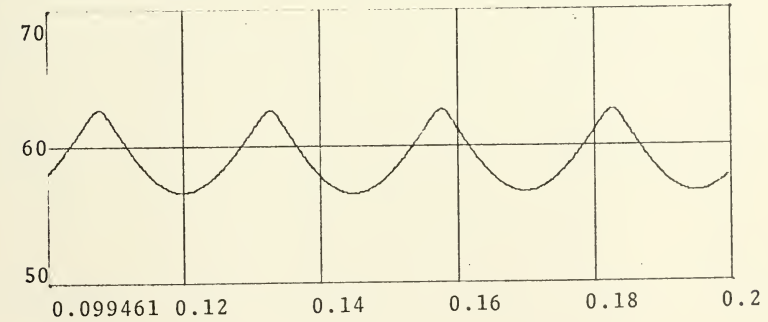

FIGURE 5.41c. Output plot, V_{ref} = 60V., R = 0.8Ω, Gain = 5.0

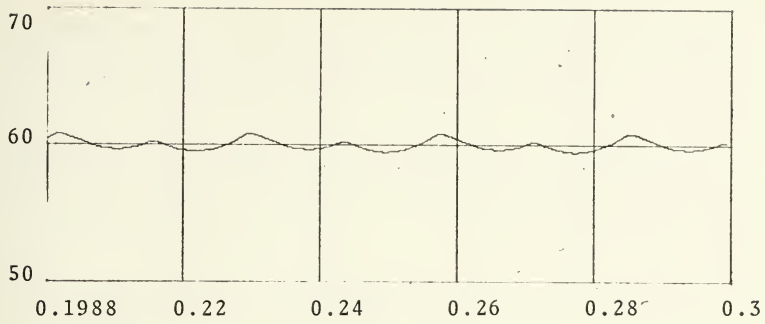

FIGURE 5.42a. Output plot, V_{ref} = 60V., R = 3.2Ω, Gain = 1000.0

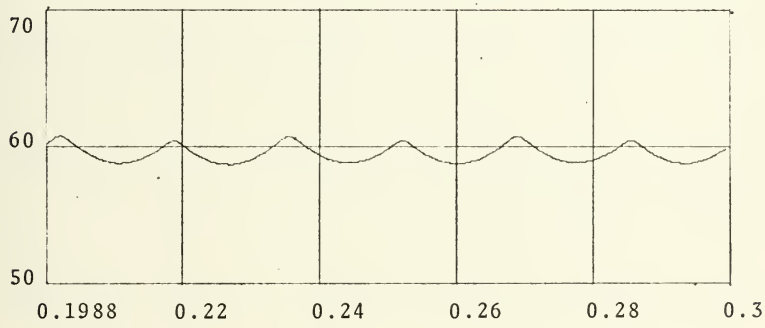

FIGURE 5.42b. Output plot, V_{ref} = 60V, R = 1.6Ω, Gain = 1000.0

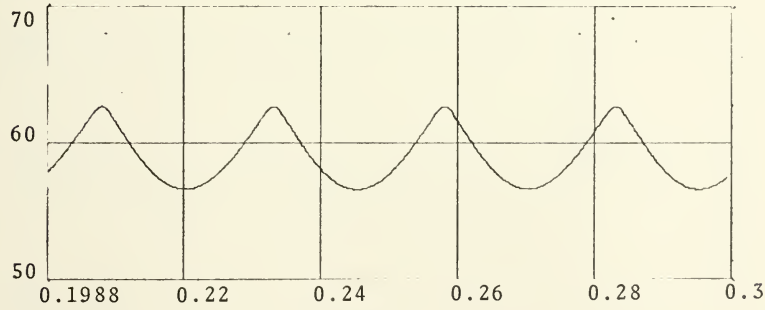

FIGURE 5.42c. Output plot, V_{ref} = 60V, R = 0.8Ω, Gain = 1000.0

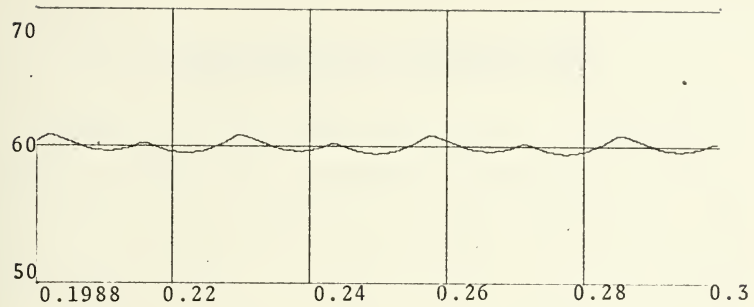

FIGURE 5.43a. Output plot, V_{ref} = 60V, R = 3.2Ω, Gain = 10,000

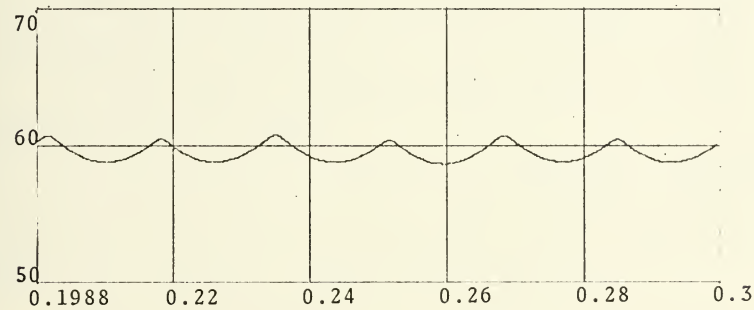

FIGURE 5.43b. Output plot, V_{ref} = 60V, R = 1.6Ω, Gain = 10,000

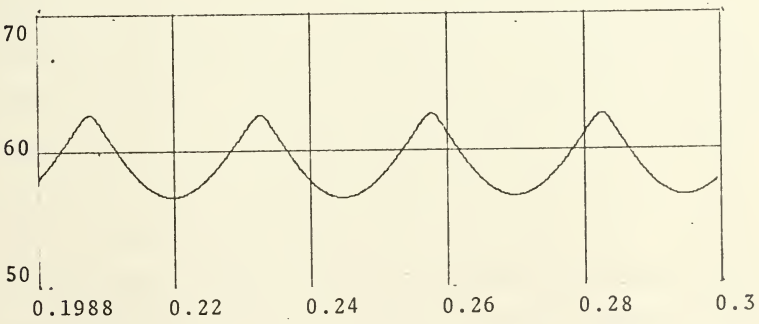

FIGURE 5.43c. Output plot, V_{ref} = 60V, R = 0.8Ω, Gain = 10,000

VI. CONCLUSIONS AND RECOMMENDATIONS

Under some load conditions a limit cycling voltage regulator system gives subharmonic resonances at the output. This is not permissible in many applications. The goal of this thesis is to investigate the voltage regulator system and to try to find out the causes of the subharmonic resonance.

Removal of the rectifier and substitution of a battery removed two basic characteristics from the system:

1. The ripple at frequency 360Hz due to the rectification of the AC supply.

2. The delayed shut-off (i.e., continued conduction after the error detector signal gave the "off" signal) due to the thyristor firing characteristics.

Since the subharmonics are observed to be submultiples of the limit cycle frequency, therefore, item (1) cannot be the cause of such subharmonics. Item (2) occurs at the limit cycle frequency, and results showed that the input voltage to the filter had a variable pulse duration for rectified AC but there was no pulse width modulation which probably caused the subharmonics. It can be seen from the input plots that the ripple begins at different voltage levels even though the system load resistance and reference voltage are held constant during

one analysis. The thyristor characteristics apparently cause this pulse width modulation.

Another important thing is the prediction of subharmonic resonance by using the Dual input Describing function. If the Dual input Describing function is derived then by designing a compensator the subharmonics may be removed from the system. As a further study, the Dual input Describing function of the nonlinearity should be derived, taking into account the pulse width modulation.

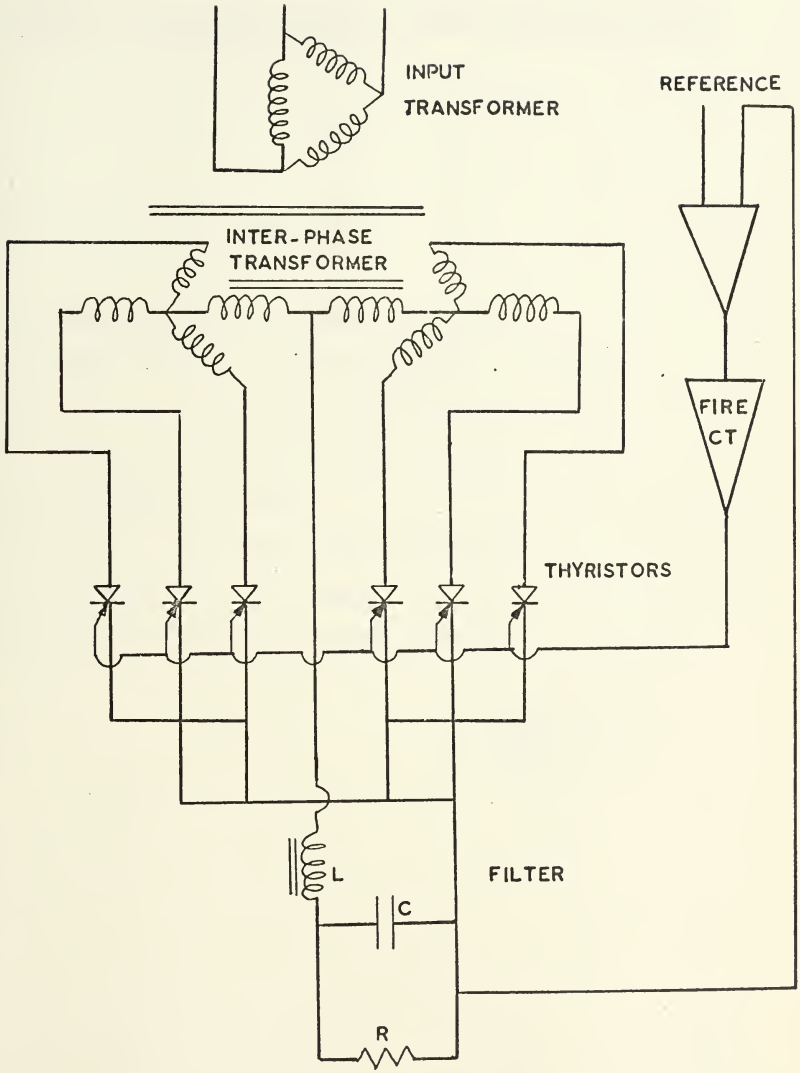

THREE PHASE, FULL WAVE, LIMIT CYCLING VOLTAGE REGULATOR

APPENDIX B: DIGITAL COMPUTER PROGRAM FOR LIMIT CYCLING VOLTAGE REGULATOR

The constants C(I) represent

C(1) = Maximum value of input sine wave

C(2) = Value of the filter inductance is henries

C(3) = Value of the filter capacitance in farads

C(4) = Value of load resistance in ohms

C(5) = Reference voltage

C(6) = Gain of amplifier before dead zone

C(7) = Magnitude of dead zone

C(8) = Gain of amplifier after dead zone

```
      DIMENSION X(30),XDOT(30),C(15)
      C(10)=1.
      IBP=1
      PI=3.141592
      X(8)=IBP
      X(10)=0.0
    1 CALL INTEG2(T,X,XDOT,C)
      X(11)=C(2)*XDOT(2)
      XMAX=C(1)*SIN(PI/3.)
      THA=2.0*PI*60.0*T
      PHASEA=ABS(C(1)*SIN(THA))
      PHASEB=ABS(C(1)*SIN(THA+2.0*PI/3.))
      PHASEC=ABS(C(1)*SIN(THA+PI/3.))
      X(6)=AMAX1(PHASEA,PHASEB,PHASEC)
      IF(PHASEA.GE.XMAX)IPH=1
      IF(PHASEB.GE.XMAX)IPH=2
      IF(PHASEC.GE.XMAX)IPH=3
  206 ERROR=X(1)-C(5)
      X(8)=IPH
      VK1=C(6)*ERROR
      IF(VK1.GE.C(7))VDZ=VK1-C(7)
      IF(VK1.LT.C(7))VDZ=0.0
      IF(VK1.LT.C.0)VDZ=VK1
      VK2=VDZ*C(8)
      GO TO(100,101,102,103,104),IBP
  100 CONTINUE
      IF(VK2) 207,207,208
  207 IBP=1
      VIN=X(6)
      X(5)=VIN
      X(7)=0.
      X(3)=(1./C(2))*(VIN-X(1))
      XDOT(2)=X(3)
      IF(X(2).LT.-0.01) X(2)=-0.01
      X(4)=(1./C(3))*X(2)-(1./(C(3)*C(4)))*X(1)
      XDOT(1)=X(4)
      VLAST=VIN
      X(8)=IBP
      GO TO 1
  208 IF(VIN.LT.VLAST) GO TO 207
      GO TO(101,102,103),IPH
  101 VIN=PHASEA
      IF(VK2)207,207,105
  105 CONTINUE
      X(7)=1.
      X(5)=VIN
      IF(VIN-.75)300,301,301
  300 VIN=0.0
      X(5)=VIN
      IBP=5
      GO TO 302
  301 IBP=2
  302 X(3)=(1./C(2))*(VIN-X(1))
      IF(X(2).LT.-0.01) X(3)=0.0
      XDOT(2)=X(3)
      IF(X(2).LT.-0.01) X(2)=-0.01
      X(4)=(1./C(3))*X(2)-(1./(C(3)*C(4)))*X(1)
      XDOT(1)=X(4)
      VLAST=VIN
      X(8)=IBP
      GO TO 1
  102 VIN=PHASEB
      IF(VK2)207,207,106
  106 CONTINUE
      X(7)=2.
      X(5)=VIN
      IF(VIN-.75)303,304,304
  303 VIN=0.0
      X(5)=VIN
      IBP=5
      GO TO 305
  304 IBP=3
  305 X(3)=(1./C(2))*(VIN-X(1))
```

```
      IF(X(2).LT.-0.01) X(3)=0.0
      XDOT(2)=X(3)
      IF(X(2).LT.-0.01) X(2)=-0.01
      X(4)=(1./C(3))*X(2)-(1./(C(3)*C(4)))*X(1)
      XDOT(1)=X(4)
      VLAST=VIN
      X(8)=IBP
      GO TO 1
  103 VIN=PHASEC
      IF(VK2)207,207,107
  107 CONTINUE
      X(7)=3.
      X(5)=VIN
      IF(VIN-.75)306,307,307
  306 VIN=0.0
      X(5)=VIN
      IBP=5
      GO TO 308
  307 IBP=4
  308 X(3)=(1./C(2))*(VIN-X(1))
      IF(X(2).LT.-0.01) X(3)=0.0
      XDOT(2)=X(3)
      IF(X(2).LT.-0.01) X(2)=-0.01
      X(4)=(1./C(3))*X(2)-(1./(C(3)*C(4)))*X(1)
      XDOT(1)=X(4)
      VLAST=VIN
      X(8)=IBP
      GO TO 1
  104 VIN=0.0
      X(7)=4.
      X(5)=VIN
      X(3)=(1./C(2))*(VIN-X(1))
      IF(X(2).LT.-0.01) X(3)=0.0
      XDOT(2)=X(3)
      IF(X(2).LT.-0.01) X(2)=-0.01
      X(4)=(1./C(3))*X(2)-(1./(C(3)*C(4)))*X(1)
      XDOT(1)=X(4)
      IBP=5
      IF(VK2)309,309,310
  309 IBP=1
  310 CONTINUE
      X(8)=IBP
      GO TO 1
      END
```

```
    GULER M.A.  FORCED LIMIT CYCLING REGULATOR  NO4
     ONE RUN IS CALLED FOR

INPUT DATA RECORD

ORDER OF EQUATIONS =  2
INITIAL TIME       = 0.0
FINAL TIME         = 0.1000E 00
STEP SIZE          = 0.2222E-04

THE NON-ZERO CONSTANTS, C(I), ARE
              C( 1) = 0.6500E 02
              C( 2) = 0.5000E-03
              C( 3) = 0.1000E 00
              C( 4) = 0.1600E 01
              C( 5) = 0.6000E 02
              C( 6) = 0.1000E 01
              C( 8) = 0.1000E 01

ALL THE INITIAL CONDITIONS ARE ZERO


THE COLUMN HEADINGS AND THE CORRESPONDING VARIABLES ARE

         TIME        X( 0)
         VIN         X( 5)
         VOUT        X( 1)
         CURRT       X( 2)


NO GRAPHS ARE REQUIRED
```

GULER M.A. FORCED LIMIT CYCLING REGULATOR NO4

TIME	VIN	VOUT	CURRT
0.0	0.56292E 02	0.0	0.0
0.44440E-03	0.60923E 02	0.11435E 00	0.52178E 02
0.88880E-03	0.63848E 02	0.46759E 00	0.10752E 03
0.13332E-02	0.64986E 02	0.10692E 01	0.16424E 03
0.17776E-02	0.64303E 02	0.19205E 01	0.22052E 03
0.22220E-02	0.61820E 02	0.30149E 01	0.27452E 03
0.26664E-02	0.57606E 02	0.43375E 01	0.32447E 03
0.31108E-02	0.59918E 02	0.58689E 01	0.37138E 03
0.35552E-02	0.63281E 02	0.76088E 01	0.42028E 03
0.39996E-02	0.64871E 02	0.95628E 01	0.46975E 03
0.44439E-02	0.64645E 02	0.11729E 02	0.51799E 03
0.48883E-02	0.62610E 02	0.14097E 02	0.56321E 03
0.53326E-02	0.58821E 02	0.16649E 02	0.60365E 03
0.57770E-02	0.58805E 02	0.19361E 02	0.63884E 03
0.62213E-02	0.62600E 02	0.22221E 02	0.67445E 03
0.66657E-02	0.64641E 02	0.25231E 02	0.71005E 03
0.71101E-02	0.64873E 02	0.28388E 02	0.74392E 03
0.75544E-02	0.63289E 02	0.31680E 02	0.77432E 03
0.79988E-02	0.59933E 02	0.35086E 02	0.79954E 03
0.84431E-02	0.57588E 02	0.38581E 02	0.81826E 03
0.88875E-02	0.61808E 02	0.42143E 02	0.83557E 03
0.93318E-02	0.64297E 02	0.45773E 02	0.85267E 03
0.97762E-02	0.64987E 02	0.49464E 02	0.86794E 03
0.10221E-01	0.63857E 02	0.53207E 02	0.87971E 03
0.10665E-01	0.60939E 02	0.56980E 02	0.88633E 03
0.11109E-01	0.56315E 02	0.60757E 02	0.88623E 03
0.11554E-01	0.50115E 02	0.64507E 02	0.87797E 03
0.11998E-01	0.42511E 02	0.68188E 02	0.86025E 03
0.12442E-01	0.33717E 02	0.71758E 02	0.83200E 03
0.12887E-01	0.23980E 02	0.75167E 02	0.79239E 03
0.13331E-01	0.13571E 02	0.78365E 02	0.74087E 03
0.13775E-01	0.27820E 01	0.81299E 02	0.67717E 03
0.14220E-01	0.0	0.83917E 02	0.60402E 03
0.14664E-01	0.0	0.86198E 02	0.52839E 03
0.15108E-01	0.0	0.88132E 02	0.45089E 03
0.15553E-01	0.0	0.89714E 02	0.37183E 03
0.15997E-01	0.0	0.90937E 02	0.29152E 03
0.16441E-01	0.0	0.91798E 02	0.21028E 03
0.16886E-01	0.0	0.92295E 02	0.12845E 03
0.17330E-01	0.0	0.92427E 02	0.46328E 02
0.17775E-01	0.0	0.92228E 02	-0.10000E-01
0.18219E-01	0.0	0.91972E 02	-0.10000E-01
0.18663E-01	0.0	0.91717E 02	-0.10000E-01
0.19108E-01	0.0	0.91462E 02	-0.10000E-01
0.19552E-01	0.0	0.91208E 02	-0.10000E-01
0.19996E-01	0.0	0.90955E 02	-0.10000E-01
0.20441E-01	0.0	0.90703E 02	-0.10000E-01
0.20885E-01	0.0	0.90451E 02	-0.10000E-01
0.21329E-01	0.0	0.90200E 02	-0.10000E-01
0.21774E-01	0.0	0.89949E 02	-0.10000E-01

GULER M.A. FORCED LIMIT CYCLING REGULATOR NO4

TIME	VIN	VOUT	CURRT
0.22218E-01	0.0	0.89700E 02	-0.10000E-01
0.22662E-01	0.0	0.89451E 02	-0.10000E-01
0.23107E-01	0.0	0.89202E 02	-0.10000E-01
0.23551E-01	0.0	0.88955E 02	-0.10000E-01
0.23995E-01	0.0	0.88708E 02	-0.10000E-01
0.24440E-01	0.0	0.88462E 02	-0.10000E-01
0.24884E-01	0.0	0.88216E 02	-0.10000E-01
0.25329E-01	0.0	0.87971E 02	-0.10000E-01
0.25773E-01	0.0	0.87727E 02	-0.10000E-01
0.26217E-01	0.0	0.87484E 02	-0.10000E-01
0.26662E-01	0.0	0.87241E 02	-0.10000E-01
0.27106E-01	0.0	0.86999E 02	-0.10000E-01
0.27550E-01	0.0	0.86757E 02	-0.10000E-01
0.27995E-01	0.0	0.86516E 02	-0.10000E-01
0.28439E-01	0.0	0.86276E 02	-0.10000E-01
0.28883E-01	0.0	0.86037E 02	-0.10000E-01
0.29328E-01	0.0	0.85798E 02	-0.10000E-01
0.29772E-01	0.0	0.85560E 02	-0.10000E-01
0.30216E-01	0.0	0.85322E 02	-0.10000E-01
0.30661E-01	0.0	0.85085E 02	-0.10000E-01
0.31105E-01	0.0	0.84849E 02	-0.10000E-01
0.31549E-01	0.0	0.84613E 02	-0.10000E-01
0.31994E-01	0.0	0.84379E 02	-0.10000E-01
0.32438E-01	0.0	0.84144E 02	-0.10000E-01
0.32883E-01	0.0	0.83911E 02	-0.10000E-01
0.33327E-01	0.0	0.83678E 02	-0.10000E-01
0.33771E-01	0.0	0.83446E 02	-0.10000E-01
0.34216E-01	0.0	0.83214E 02	-0.10000E-01
0.34660E-01	0.0	0.82983E 02	-0.10000E-01
0.35104E-01	0.0	0.82753E 02	-0.10000E-01
0.35549E-01	0.0	0.82523E 02	-0.10000E-01
0.35993E-01	0.0	0.82294E 02	-0.10000E-01
0.36437E-01	0.0	0.82065E 02	-0.10000E-01
0.36882E-01	0.0	0.81837E 02	-0.10000E-01
0.37326E-01	0.0	0.81610E 02	-0.10000E-01
0.37770E-01	0.0	0.81384E 02	-0.10000E-01
0.38215E-01	0.0	0.81158E 02	-0.10000E-01
0.38659E-01	0.0	0.80932E 02	-0.10000E-01
0.39103E-01	0.0	0.80708E 02	-0.10000E-01
0.39548E-01	0.0	0.80484E 02	-0.10000E-01
0.39992E-01	0.0	0.80260E 02	-0.10000E-01
0.40436E-01	0.0	0.80038E 02	-0.10000E-01
0.40881E-01	0.0	0.79815E 02	-0.10000E-01
0.41325E-01	0.0	0.79594E 02	-0.10000E-01
0.41770E-01	0.0	0.79373E 02	-0.10000E-01
0.42214E-01	0.0	0.79152E 02	-0.10000E-01
0.42658E-01	0.0	0.78933E 02	-0.10000E-01
0.43103E-01	0.0	0.78714E 02	-0.10000E-01
0.43547E-01	0.0	0.78495E 02	-0.10000E-01
0.43991E-01	0.0	0.78277E 02	-0.10000E-01

GULER M.A. FORCED LIMIT CYCLING REGULATOR NO4

TIME	VIN	VOUT	CURRT
0.44436E-01	0.0	0.78060E 02	-0.10000E-01
0.44880E-01	0.0	0.77843E 02	-0.10000E-01
0.45324E-01	0.0	0.77627E 02	-0.10000E-01
0.45769E-01	0.0	0.77412E 02	-0.10000E-01
0.46213E-01	0.0	0.77197E 02	-0.10000E-01
0.46657E-01	0.0	0.76982E 02	-0.10000E-01
0.47102E-01	0.0	0.76769E 02	-0.10000E-01
0.47546E-01	0.0	0.76555E 02	-0.10000E-01
0.47990E-01	0.0	0.76343E 02	-0.10000E-01
0.48435E-01	0.0	0.76131E 02	-0.10000E-01
0.48879E-01	0.0	0.75920E 02	-0.10000E-01
0.49324E-01	0.0	0.75709E 02	-0.10000E-01
0.49768E-01	0.0	0.75499E 02	-0.10000E-01
0.50212E-01	0.0	0.75289E 02	-0.10000E-01
0.50657E-01	0.0	0.75080E 02	-0.10000E-01
0.51101E-01	0.0	0.74872E 02	-0.10000E-01
0.51545E-01	0.0	0.74664E 02	-0.10000E-01
0.51990E-01	0.0	0.74456E 02	-0.10000E-01
0.52434E-01	0.0	0.74250E 02	-0.10000E-01
0.52878E-01	0.0	0.74044E 02	-0.10000E-01
0.53323E-01	0.0	0.73838E 02	-0.10000E-01
0.53767E-01	0.0	0.73633E 02	-0.10000E-01
0.54211E-01	0.0	0.73429E 02	-0.10000E-01
0.54656E-01	0.0	0.73225E 02	-0.10000E-01
0.55100E-01	0.0	0.73021E 02	-0.10000E-01
0.55544E-01	0.0	0.72819E 02	-0.10000E-01
0.55989E-01	0.0	0.72617E 02	-0.10000E-01
0.56433E-01	0.0	0.72415E 02	-0.10000E-01
0.56878E-01	0.0	0.72214E 02	-0.10000E-01
0.57322E-01	0.0	0.72013E 02	-0.10000E-01
0.57766E-01	0.0	0.71813E 02	-0.10000E-01
0.58211E-01	0.0	0.71614E 02	-0.10000E-01
0.58655E-01	0.0	0.71415E 02	-0.10000E-01
0.59099E-01	0.0	0.71217E 02	-0.10000E-01
0.59544E-01	0.0	0.71019E 02	-0.10000E-01
0.59988E-01	0.0	0.70822E 02	-0.10000E-01
0.60432E-01	0.0	0.70625E 02	-0.10000E-01
0.60877E-01	0.0	0.70429E 02	-0.10000E-01
0.61321E-01	0.0	0.70234E 02	-0.10000E-01
0.61765E-01	0.0	0.70039E 02	-0.10000E-01
0.62210E-01	0.0	0.69844E 02	-0.10000E-01
0.62654E-01	0.0	0.69650E 02	-0.10000E-01
0.63097E-01	0.0	0.69457E 02	-0.10000E-01
0.63541E-01	0.0	0.69264E 02	-0.10000E-01
0.63984E-01	0.0	0.69072E 02	-0.10000E-01
0.64428E-01	0.0	0.68880E 02	-0.10000E-01
0.64871E-01	0.0	0.68689E 02	-0.10000E-01
0.65315E-01	0.0	0.68498E 02	-0.10000E-01
0.65758E-01	0.0	0.68308E 02	-0.10000E-01
0.66202E-01	0.0	0.68118E 02	-0.10000E-01

GULER M.A. FORCED LIMIT CYCLING REGULATOR NO4

TIME	VIN	VOUT	CURRT
0.66645E-01	0.0	0.67929E 02	-0.10000E-01
0.67088E-01	0.0	0.67741E 02	-0.10000E-01
0.67532E-01	0.0	0.67552E 02	-0.10000E-01
0.67975E-01	0.0	0.67365E 02	-0.10000E-01
0.68419E-01	0.0	0.67178E 02	-0.10000E-01
0.68862E-01	0.0	0.66991E 02	-0.10000E-01
0.69306E-01	0.0	0.66805E 02	-0.10000E-01
0.69749E-01	0.0	0.66620E 02	-0.10000E-01
0.70193E-01	0.0	0.66435E 02	-0.10000E-01
0.70636E-01	0.0	0.66250E 02	-0.10000E-01
0.71080E-01	0.0	0.66066E 02	-0.10000E-01
0.71523E-01	0.0	0.65883E 02	-0.10000E-01
0.71966E-01	0.0	0.65700E 02	-0.10000E-01
0.72410E-01	0.0	0.65518E 02	-0.10000E-01
0.72853E-01	0.0	0.65336E 02	-0.10000E-01
0.73297E-01	0.0	0.65154E 02	-0.10000E-01
0.73740E-01	0.0	0.64973E 02	-0.10000E-01
0.74184E-01	0.0	0.64793E 02	-0.10000E-01
0.74627E-01	0.0	0.64613E 02	-0.10000E-01
0.75071E-01	0.0	0.64434E 02	-0.10000E-01
0.75514E-01	0.0	0.64255E 02	-0.10000E-01
0.75958E-01	0.0	0.64076E 02	-0.10000E-01
0.76401E-01	0.0	0.63898E 02	-0.10000E-01
0.76845E-01	0.0	0.63721E 02	-0.10000E-01
0.77288E-01	0.0	0.63544E 02	-0.10000E-01
0.77731E-01	0.0	0.63368E 02	-0.10000E-01
0.78175E-01	0.0	0.63192E 02	-0.10000E-01
0.78618E-01	0.0	0.63016E 02	-0.10000E-01
0.79062E-01	0.0	0.62841E 02	-0.10000E-01
0.79505E-01	0.0	0.62667E 02	-0.10000E-01
0.79949E-01	0.0	0.62493E 02	-0.10000E-01
0.80392E-01	0.0	0.62319E 02	-0.10000E-01
0.80836E-01	0.0	0.62146E 02	-0.10000E-01
0.81279E-01	0.0	0.61974E 02	-0.10000E-01
0.81723E-01	0.0	0.61802E 02	-0.10000E-01
0.82166E-01	0.0	0.61630E 02	-0.10000E-01
0.82609E-01	0.0	0.61459E 02	-0.10000E-01
0.83053E-01	0.0	0.61288E 02	-0.10000E-01
0.83496E-01	0.0	0.61118E 02	-0.10000E-01
0.83940E-01	0.0	0.60948E 02	-0.10000E-01
0.84383E-01	0.0	0.60779E 02	-0.10000E-01
0.84827E-01	0.0	0.60610E 02	-0.10000E-01
0.85270E-01	0.0	0.60442E 02	-0.10000E-01
0.85714E-01	0.0	0.60274E 02	-0.10000E-01
0.86157E-01	0.0	0.60107E 02	-0.10000E-01
0.86601E-01	0.61298E 02	0.59940E 02	-0.10000E-01
0.87044E-01	0.64042E 02	0.59776E 02	0.19466E 01
0.87488E-01	0.64999E 02	0.59628E 02	0.63648E 01
0.87931E-01	0.64144E 02	0.59501E 02	0.10951E 02
0.88374E-01	0.61501E 02	0.59392E 02	0.14083E 02

GULER M.A. FORCED LIMIT CYCLING REGULATOR NO4

TIME	VIN	VOUT	CURRT
0.88818E-01	0.57142E 02	0.59291E 02	0.14188E 02
0.89261E-01	0.60285E 02	0.59186E 02	0.13191E 02
0.89705E-01	0.63489E 02	0.59085E 02	0.15766E 02
0.90148E-01	0.64922E 02	0.59001E 02	0.20489E 02
0.90592E-01	0.64546E 02	0.58940E 02	0.25748E 02
0.91035E-01	0.62369E 02	0.58901E 02	0.29914E 02
0.91479E-01	0.58454E 02	0.58874E 02	0.31394E 02
0.91922E-01	0.59155E 02	0.58847E 02	0.30281E 02
0.92366E-01	0.62813E 02	0.58822E 02	0.32318E 02
0.92809E-01	0.64719E 02	0.58811E 02	0.36851E 02
0.93252E-01	0.64821E 02	0.58823E 02	0.42278E 02
0.93696E-01	0.63116E 02	0.58859E 02	0.46969E 02
0.94139E-01	0.59650E 02	0.58910E 02	0.49318E 02
0.94583E-01	0.57909E 02	0.58964E 02	0.48260E 02
0.95026E-01	0.62014E 02	0.59015E 02	0.49249E 02
0.95470E-01	0.64390E 02	0.59078E 02	0.53074E 02
0.95913E-01	0.64971E 02	0.59160E 02	0.58153E 02
0.96357E-01	0.63739E 02	0.59265E 02	0.62858E 02
0.96800E-01	0.60731E 02	0.59387E 02	0.65574E 02
0.97244E-01	0.56550E 02	0.59513E 02	0.64756E 02
0.97687E-01	0.61094E 02	0.59632E 02	0.64211E 02
0.98131E-01	0.63936E 02	0.59756E 02	0.66849E 02
0.98574E-01	0.64994E 02	0.59896E 02	0.71106E 02
0.99017E-01	0.64239E 02	0.60055E 02	0.75366E 02
0.99461E-01	0.61694E 02	0.60230E 02	0.78007E 02

AT 4500 INTEGRATION STEPS

ONE RUN CALLED FOR HAS BEEN COMPLETED.

APPENDIX C

SUMMER AMPLIFIER:

Amplifiers on the patch board are addressed as an even number A000 to A126, and are represented with a gain symbol at the input to the amplifier

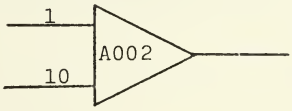

INVERTERS:

Sign changes are addressed from A200 to A217 and are represented as

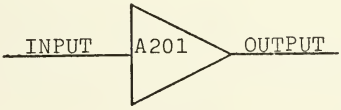

INTEGRATOR:

These amplifiers are addressed on the patch board as odd numbers (A001 to A047) and are integrators. They are represented with a symbol

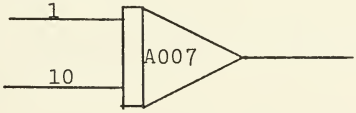

A007 and A011 were used.

COMPARATOR:

A kind of device which gives Ov. or -6v. logic level according to the comparison of the inputs. Represented with symbol

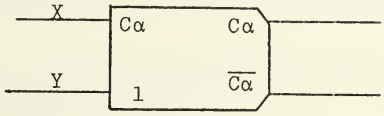

such that if

$$X+Y > o \begin{cases} C_\alpha = -6v. \\ \overline{C_\alpha} = 0v. \end{cases}$$

$$X+Y < o \begin{cases} C_\alpha = 0v. \\ \overline{C_\alpha} = -6v. \end{cases}$$

DIGITAL/ANALOG SWITCH (DA):

It is a switch and is represented with a symbol

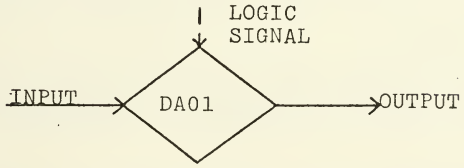

The switch is closed if logic signal is -6v. and open if logic signal is Ov. These logic levels usually come from a comparator. Switching time is approximately equal to 1 μsec.

LIST OF REFERENCES

1. Thaler, G. J. and Brown, R. G., Analysis and Design of Feedback Control System, McGraw-Hill, 1960.

2. Thaler, G. J. and Pastel, M. P., Analysis and Design of Nonlinear Feedback Control Systems, McGraw-Hill, 1962.

3. Gelb, A. and Vander Velde, W. E., Multiple-Input Describing Functions on Nonlinear System Design, McGraw-Hill, 1968.

4. West, J. C., Analytical Techniques for Nonlinear Control Systems, VanNostrand, 1960.

5. Hayashi, C., Nonlinear Oscillation in Physical Systems, McGraw-Hill, 1964.

6. Poole, S. and Jackson, P. A., Electrical Control Engineering, Vol. 1, London ILIFEE, 1967.

7. Gelb, A., "The Analysis and Design of Limit Cycling Adaptive Automatic Control Systems", Doctoral Dissertation, MIT, 1961.

8. Edwards, D. L., Gass, A. E., Thaler, G. J., and Trubell, L. P., "Stability Analysis of Phase Controlled Regulators", IBM Machine Technology Report, 14 May 1963.

9. West, J. C., Douce, J. L., and Livesley, R. K., The Dual-Input Describing Function and Its Use in the Analysis of Nonlinear Feedback System, Proc. of IEEE, Vol. 103, par. B, p. 463, July 1955.

10. West, J. C. and Douce, J. L., Mechanism of Subharmonic Generation in a Feedback System, Proc. of IEEE, Vol. 102, p. 563, July 1954.

11. Gibson, J. E., and Sirdhar, A New Dual-Input Describing Function and an Application to the Stability of Forced Nonlinear Systems, Trans. AIEE, p. 65-70, May 1963.

12. Gibson, J. E., A New Dual-Input Describing Function and an Application to the Stability of Forced Nonlinear Systems, Trans. AIEE, p. 1-6.

13. Gelb, A. and Vander Velde, W. E., On Limit Cycling Control Systems, Trans. IEEE. Autom. Control, p. 142-157, April 1963.

14. Gelb, A., The Dynamic Input-Output Analysis of Limit Cycling Control Systems, Proc. JACC, p. 3.3-1-3.3-11, June 1962.

15. Leszcynski, V. J., Analysis of a Forced Limit-Cycling Regulator, Thesis, Naval Postgraduate School, 1968.

16. Hyde, W. H., Jr., Investigation of Subharmonic Ripple in a Forced Limit-Cycling Regulator, Thesis, Naval Postgraduate School, 1968.

INITIAL DISTRIBUTION LIST

		No. Copies
1.	Defense Documentation Center Cameron Station Alexandria, Virginia 22314	2
2.	Library, Code 0212 Naval Postgraduate School Monterey, California 93940	2
3.	Deniz K. K. Personel Eğitim Sb. Müdürlügü Ankara, Turkey	1
4.	Deniz Harb Okulu K. Heybeliada, Istanbul Turkey	1
5.	Dr. G. J. Thaler (thesis advisor) Department of Electrical Engineering Naval Postgraduate School Monterey, California 93940	10
6.	Istanbul Teknik Universitesi Elektrik Fakultesi Taskisla, Istanbul Turkey	1
7.	Lt. j.g. M. Ali Güler Zulalecesme sok No. 2/3 Fatih-Istanbul Turkey	4

DOCUMENT CONTROL DATA - R & D

(Security classification of title, body of abstract and indexing annotation must be entered when the overall report is classified)

1. ORIGINATING ACTIVITY *(Corporate author)*
Naval Postgraduate School
Monterey, California 93940

2a. REPORT SECURITY CLASSIFICATION
UNCLASSIFIED

2b. GROUP

3. REPORT TITLE
Subharmonic Resonance in a Limit Cycling Voltage Regulator

4. DESCRIPTIVE NOTES *(Type of report and, inclusive dates)*
Master's Thesis, December 1970

5. AUTHOR(S) *(First name, middle initial, last name)*
M. Ali Güler

6. REPORT DATE	7a. TOTAL NO. OF PAGES	7b. NO. OF REFS
December 1970	107	16

8a. CONTRACT OR GRANT NO.	9a. ORIGINATOR'S REPORT NUMBER(S)
b. PROJECT NO.	
c.	9b. OTHER REPORT NO(S) *(Any other numbers that may be assigned this report)*
d.	

10. DISTRIBUTION STATEMENT
This document has been approved for public release and sale; its distribution is unlimited.

11. SUPPLEMENTARY NOTES	12. SPONSORING MILITARY ACTIVITY
	Naval Postgraduate School Monterey, California 93940

13. ABSTRACT

In practice, thyristor rectifiers are used as high current-low power supplies. Under certain conditions such rectifiers introduce subharmonic resonances.

In this paper, a limit cycling voltage regulator system is simulated in the digital computer. The reference voltage and load are varied and the system gain is changed for better understanding of their effects on the subharmonics. A Fourier analysis of the output wave shape then determined the existence and amplitude of subharmonic components.

14 KEY WORDS	LINK A		LINK B		LINK C	
	ROLE	WT	ROLE	WT	ROLE	WT
Subharmonic Resonance						
Limit Cycling						
Dual Input Describing Function						

Thesis
G86366
c.1

125668

Güler
Subharmonic resonance in a limit cycling voltage regulator.